

Analog Integrated Circuits  
**TITOLO SERIO**

Roberto Rr  
chopper19

DATA



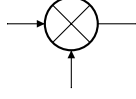
# Contents

|          |   |           |
|----------|---|-----------|
| <b>1</b> | <b>Introduction</b>   | <b>1</b>  |
| <b>2</b> | <b>Analysis of a Gilbert cell-based multiplier</b>                                  | <b>6</b>  |
| 2.1      | Gilbert cell overview . . . . .   | 6         |
| 2.2      | Gilbert cell circuit analysis . . . . .   | 7         |
| 2.3      | Mathematical analysis: conversion gain . . . . .                                    | 13        |
| <b>3</b> | <b>Design by hand of a down-converting Gilbert cell</b>                             | <b>18</b> |
| 3.1      | Design specifications . . . . .   | 18        |
| 3.2      | Gilbert cell design flow . . . . .  | 19        |
| <b>4</b> | <b>Design by simulation</b>   | <b>22</b> |
| 4.1      | Gilbert Cell design . . . . .   | 22        |
| 4.2      | Biasing network design . . . . .  | 26        |
| <b>5</b> | <b>Layout of the Gilbert Cell</b>   | <b>28</b> |
| 5.1      | Differential RF stage . . . . .   | 28        |
| 5.2      | Differential LO stages . . . . .  | 30        |
| 5.3      | Current mirror and diode connected transistor . . . . .                             | 30        |
| 5.4      | Capacitors . . . . .  | 32        |
| 5.5      | Resistors . . . . .   | 34        |
| 5.6      | Putting together the layout . . . . .   | 36        |
| <b>6</b> | <b>Simulation vs schematic comparison</b>   | <b>38</b> |
| 6.1      | Simulation setup . . . . .  | 38        |
| 6.2      | Time domain mixed signal . . . . .  | 41        |
| 6.3      | Maximum conversion gain vs LO . . . . .   | 42        |
| 6.4      | Conversion gain and 1dB compression point . . . . .                                 | 42        |
| 6.5      | Single tone third order distortion . . . . .  | 44        |
| 6.6      | Two tone IM <sub>3</sub> and CIM <sub>3</sub> ratio . . . . .                       | 47        |
| 6.7      | Bandwidth and CMRR of RF stage (output node filtering,<br>current mixing) . . . . . | 51        |
| 6.8      | pavarotti? . . . . .  | 52        |
| <b>7</b> | <b>Conclusions</b>  | <b>53</b> |



**DA SISTEMARE** There are many deadlocks and dependencies which have to be taken into consideration while designing the specifications for the transistors in order to satisfy the above design constraints. All the calculated values are changed based on the parametric analysis of transistors in Cadence Virtuoso.





## 1 Introduction

An analog multiplier, also known as mixer, is a circuit that performs the product between two signals. As we will see, this feature can be exploited to convert informations from a certain frequency band to another by means of the intrinsic non-linear behaviour of this net. Supposing to have two sinusoidal signals

$$\begin{aligned}x_1(t) &= A_1 \cos(\omega_1 t + \varphi_1) \\x_2(t) &= A_2 \cos(\omega_2 t + \varphi_2)\end{aligned}$$

and the ideal mixer shown in **figure one** has that the out-coming signal  $y(t)$  is given by:

$$\begin{aligned}y(t) &= x_1(t) \cdot x_2(t) \\&= A_1 A_2 \cos(\omega_1 t + \varphi_1) \cos(\omega_2 t + \varphi_2) \\&= \frac{A_1 A_2}{2} \{ \cos[(\omega_1 - \omega_2)t + \varphi_1 - \varphi_2] + \cos[(\omega_1 + \omega_2)t + \varphi_1 + \varphi_2] \} \\&= A \cos(\omega_{LF} t + \varphi_{LF}) + A \cos(\omega_{HF} t + \varphi_{HF})\end{aligned}$$

where

$$\begin{aligned}\omega_{LF} &= |\omega_1 - \omega_2| \\ \omega_{HF} &= |\omega_1 + \omega_2| \\ \varphi_{LF} &= \varphi_1 - \varphi_2 \\ \varphi_{HF} &= \varphi_1 + \varphi_2\end{aligned}$$

Therefore, it comes that two signals with different frequency allocation are obtained at the output port: the former at  $\omega_{LF} < \omega_1, \omega_2$  will be the down-converted component whereas the latter, with  $\omega_{HF} > \omega_1, \omega_2$ , will be the up-converted one. Moreover, it is possible to select only one of these two signals by properly filtering out the unwanted part. Overall one can read the process as a modulation of an input signal by means of a carrier. Since the mixer is a bidirectional three-port, one can distinguish:

- The high frequency signal, RF. In case of down-conversion this is one input of the circuit, vice-versa it is the output (after filtering).
- The intermediate frequency signal, IF. In case of up-conversion this is one input of the circuit, vice-versa it is the output (after filtering).

- The local oscillator, LO. This is the carrier and it is always an input with known frequency.

Based on the above, it turns out that to mix-up two signals a non-linear device is needed, since the input components are at different frequency with respect to the output and a non-linear relation between voltages and currents appears. In general, mixing can be carried out by time-varying systems that can be implemented using:

**passive devices** typically switches (diodes and transistors). In this case the mixing process introduces a *loss* since the output power is always less than the input one.

**active devices** amplifying devices are used in active region providing *gain*.<sup>1</sup> They are more power consuming and less noisy than passive mixers.

Another way to classify mixers is the following:

**Single balanced mixers** One or both input signals can pass to output, but it is not possible to suppress both of them,

**Double balanced mixers** Thanks to symmetry in the net both the input and the LO are rejected at the output port. They show better isolation between ports than SBM.

To understand why a transistors can be used, let's consider the non-linear quadratic model for a nMOSFET, supposing to drive that by injecting a two tone signal  $v_{GS}(t) = v_{RF}(t) + v_{LO}(t)$  at the gate (down-conversion configuration). One has:

$$\begin{aligned} i_D(t) &= k(v_{GS}(t) - V_{th})^2 \\ &= k(v_{RF}(t) + v_{LO}(t) - V_{th})^2 \\ &= k[v_{RF}^2(t) + v_{LO}^2(t) + 2v_{RF}(t)v_{LO}(t) - 2(v_{RF}(t) + v_{LO}(t))V_{th} + V_{th}^2] \end{aligned}$$

Supposing now  $v_{RF} \ll v_{LO}$ :

$$\begin{aligned} i_D(t) &\simeq k(v_{LO}(t) - V_{th})^2 + 2k(v_{LO}(t) - V_{th})v_{RF}(t) \\ &= I_D(t) + g_m(t)v_{RF}(t) \end{aligned}$$

hence, the model becomes a *quasi-linear* time-varying *small signal model* and the device operates in the *Small Signal Large Signal* regime (SSLS), because we still have the product of the two input signals through the transconductance. It is worth it to notice that depending on the amplitude of the RF (the LO is always driven in large signal), mixing can be obtained both in linear region or through second order non-linearity (fully non-linear

---

<sup>1</sup>The definition of the gain and loss in mixer will be presented further.



device). A more detailed analysis about how to drive a mixer follows in section 2.

Similarly to linear circuits, even in case of mixers it is possible to define the gain. Actually, gain is defined only in case of linear systems, but this figure of merit is necessary to qualify the performance of the conversion stage. In case of non-monochromatic signals (general case) one defines the *voltage conversion gain* as:

$$A_v = \frac{V_{IF,rms}}{V_{RF,rms}}$$

moreover, one has that the output power is proportional to LO power (that is also called a *pump*), even if this dependency does not appear explicitly.

An important figure of merit concerning mixers is given by the -1dB compression point of the  $P_{in}/P_{out}$  characteristic. By increasing the value of the RF signal, the amount of harmonics at the output besides the fundamental IF frequency increases as well, eventually saturating the output signals (gain compression or flatness). This is due to the fact that power is no more mainly carried by the fundamental output tone (i.e. the IF tone), but it is rather shared by all the growing up harmonics. In other words the conversion gain stops to be constant, reduces and the output waveform is clipped. Supposing to have input and output impedance matching one has that:

$$\begin{aligned} A_{conv} &= \frac{P_{IF}}{P_{RF}} \\ 10 \log_{10} A_{conv} &= 10 \log_{10} \frac{P_{IF}}{P_{RF}} \\ 10 \log_{10} P_{IF} &= 10 \log_{10} A_{conv} + 10 \log_{10} P_{RF} \\ P_{IF}|_{dB_m} &= A_{conv}|_{dB} + P_{RF}|_{dB_m} + 30dB \end{aligned}$$

This suggests both that the ideal output characteristic looks linear in log scale until the gain does not compress and that the -1dB compression point can be defined as the output IF voltage at which:

$$P_{IF}|_{-1dB} = A_{conv}|_{dB} + P_{RF}|_{dB_m} - 1dB$$

hence:

$$P_{IF}|_{-1dB} = P_{IF}|_{dB_m,ideal} - 1dB$$

Other figures of merit, that play the most important role in defining the 1dB compression point, concern the third order distortions, that can be defined as follow:

**Third Order Distortion** In this case the input is a monochromatic signal. Because of the intrinsic device's non-linearity, the output signal contains frequency components not present at the input. It can be demonstrated that the most important spurious contribution on output fundamental

tone comes from the third order term, in fact, by expanding the device's output current in Taylor's series and supposing a monochromatic gate signal, one has:

$$\begin{aligned} i_D(t) &= I_D|_{V_{GS}} + av_{gs}(t) + bv_{gs}^2(t) + cv_{gs}^3(t) + \dots \\ &= I_D|_{V_{GS}} + i_{D,fund}(t) + i_{D,SOD}(t) + i_{D,TOD}(t) + \dots \end{aligned} \quad (1)$$

Where  $a > b > c$ , meaning that increasing input signal strength each element will be more important. Developing the first three terms of the series expansion one has:

$$i_{D,fund}(t) \propto a \cos(\omega_0 t) \quad (2)$$

$$i_{D,SOD}(t) \propto b \cos^2(\omega_0 t) = \frac{1}{2}b + \frac{1}{2}b \cos(2\omega_0 t) \quad (3)$$

$$i_{D,TOD}(t) \propto c \cos^3(\omega_0 t) = \frac{3}{4}c \cos(\omega_0 t) + \frac{1}{4}c \cos(3\omega_0 t) \quad (4)$$

It is straightforward that the third order term yields an additive contribution exactly at the fundamental tone, whereas the second order distortion adds a zero-frequency term that is not damaging (a balanced configuration can reject this signal part). In general, even order distortions (2<sup>nd</sup>, 4<sup>th</sup> ...) contributes in corrupt the output signals as well, they are less important though. Also 5<sup>th</sup> order distortion exist, for which the same reasonings hold. Since the whole signal is mixed, all the additional tones introduced by distortion are converted and they may produce in-band spurious components.

**Third Order Intermodulation, CIM<sub>3</sub>** This distortion comes from a two-tone input injection ( $f_1 = f_0$  and  $f_2 = f_0 + \delta f$ ). Due to intermodulation between tones, spurious frequencies are generated. The most important contribution comes from the third order intermodulation (IM3):  $|m| + |n| = 3$  and  $mn < 0$  (where  $m = \pm 2, \pm 1$  and  $n = \pm 2, \pm 1$  are the intermodulation indexes). Taking  $m = 2$  and  $n = -1$ :

$$f_{IM3|m=2,n=-1} = 2f_1 - f_2 = f_0 - \delta f$$

that is clearly an in-band distortion. It can be demonstrated (FONTE) that, in case of same input and output reference impedance, the out and in intermodulation points are related to stage gain and output power of first harmonic:

$$\begin{aligned} OIP_3|_{dB} &= \frac{3}{2}P_{out,1st}|_{dB} - \frac{1}{2}P_{out,IM3}|_{dB} \\ IIP_3|_{dB} &= OIP_3|_{dB} - A_{v,1st}|_{dB} \end{aligned}$$

By taking  $m = -1$  and  $n = 2$  one has instead:

$$f_{IM3|m=-1,n=2} = -f_1 + 2f_2 = f_0 + \delta f$$

We notice that the whole spectrum presents side-bands produced by intermodulation. This phenomenon is called *spectra regrowth* and it can be quantified by the *Carrier to Intermodulation Ratio*. In case of mixing we change frequency band from input to output, anyway the previous result holds:

$$f_{IF,IM3}|_{m=2,n=-1} = 2f_{RF1} - f_{RF2} - f_{LO} = f_{IF} - \delta f$$

**DA FINIRE CON FIGURE DI MERITO**

## 2 Analysis of a Gilbert cell-based multiplier

### 2.1 Gilbert cell overview

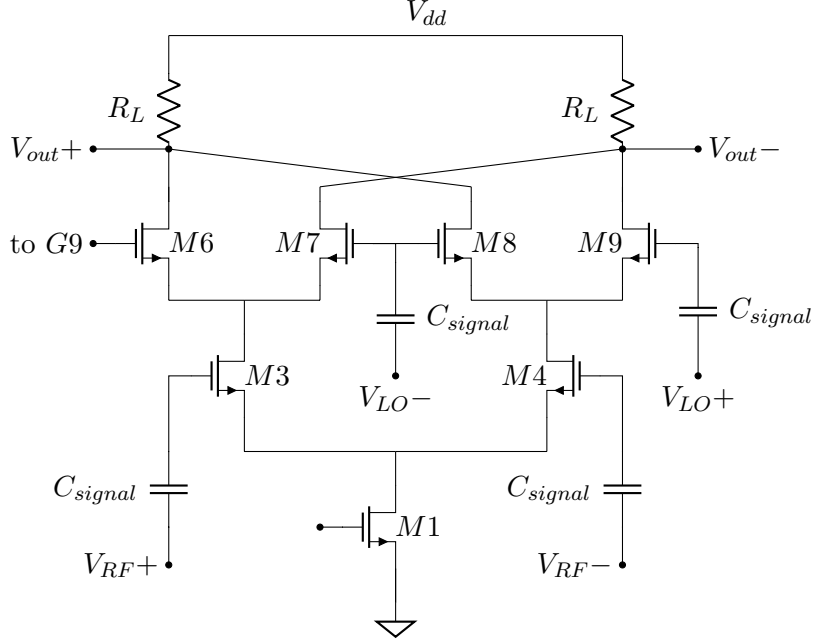


**Figure 1:** Gilbert cell mixer

A CMOS-based technology Gilbert cell-based mixer is shown in figure 1, whereas the biasing network can be found in figure 2. This circuit exploits a differential topology to implement a double-balanced cell, providing:

- Reasonable conversion gain (from one to some tens);
- Good input frequency rejection components to the output port along with high linearity, thanks to the double-balanced topology if performs;<sup>2</sup>
- Good isolation between ports is provided by the high suppression of spurious frequency components;
- Possibility of integration thanks to the CMOS architecture.

<sup>2</sup>The linearity is meant with respect to the conversion gain.

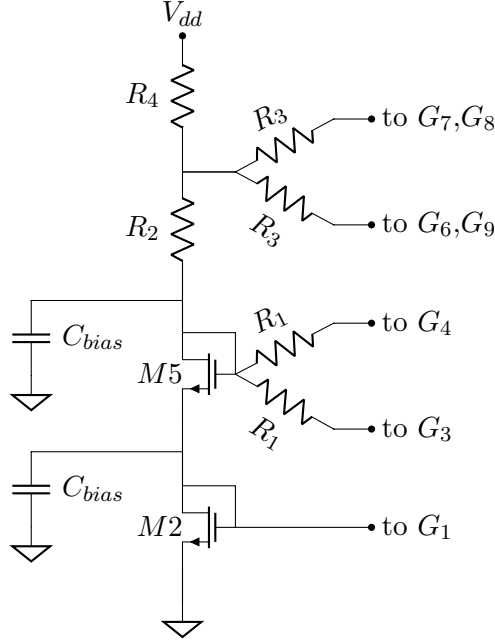


**Figure 2:** Biasing network

## 2.2 Gilbert cell circuit analysis

To analyse the circuit it is necessary to give some informations about its topology, biasing and driving. Looking at figure 1 and 2 it is possible to identify five main blocks that are described in what follows.

**Bias net** This net is made up of the current mirror (transistors M1 and M2, figure 3) and the voltage reference generation branch (transistor M5, R1, R2, R3, R4, R5; figure 2).

Transistor M1 is the strong branch of the current mirror and it acts as a current sink for the differential pair made up by M3 and M4, fixing the biasing current for the whole circuit. M2 sinks instead the current from the voltage reference section of the bias net. Generally transistors in current mirrors are polarized in saturation region, so that an high output resistance is seen from the stage above: this means that M1 should appear as a good current sink. Given  $V_{G1} = V_{GS1}$  the gate voltage in M1 we have that the transistor remains in saturation if:

$$V_{GS} \geq V_{th} \quad (5)$$

$$V_{DS} > V_{od} = V_{GS} - V_{th} \quad (6)$$

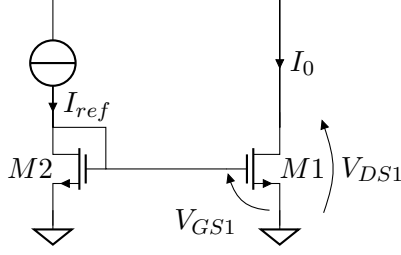


**Figure 3:** Current mirror

The same holds for M2, that is always in saturation condition since it is diode connected (provided 5). In saturation (neglecting channel modulation effects), one has that the drain current only depends on gate voltage and it is given by:

$$I_D = \mu_{n,eff} \frac{C_{ox}}{2} \frac{W}{L} (V_{GS} - V_{th})^2 = \frac{\beta_n}{2} V_{od}^2 \quad (7)$$

hence M1 remains in saturation till when:

$$V_{DS1} \geq V_{od1} = V_{th} - \sqrt{\frac{2I_0}{\beta_n}} \quad (8)$$

therefore to have a low value of the overdrive voltage one should have large transistors, i.e. large  $W$ . The output resistance is instead defined by:

$$r_o = \frac{1}{\lambda I_0} \propto L \quad (9)$$

where  $\lambda$  takes count of the channel modulation. It appears that we need long transistors to have better current sinking properties. By looking at FIGURE 2, one has (supposing both M2 and M1 in saturation, and  $V_{GS1} = V_{GS2} = V_{DS1} = V_{DS2}$ ):

$$I_0 = \frac{\beta_{n1}}{2} (V_{GS1} - V_{th})^2 (1 + \lambda_1 V_{DS1})$$

$$I_{REF} = \frac{\beta_{n2}}{2} (V_{GS1} - V_{th})^2 (1 + \lambda_1 V_{GS1})$$

hence, supposing to have equal transistors:

$$\frac{I_0}{I_{REF}} = \frac{W_1/L_1}{W_2/L_2} \quad (10)$$

Ideally the current mirroring is only depending on geometrical parameters, meaning that a very good matching is required. Even if the two devices are very close to each other within the same chip, the possibility to have a variation in parameters that depend on temperature exists, i.e.  $V_{th}$  and  $\mu_{n,eff}$ . Supposing to have equal devices with everything constant but:

$$K_{n1} = K_n + \Delta K_n$$

$$V_{th,1} = V_{th} + \Delta V_{th}$$

one eventually finds that:

$$\frac{I_0}{I_{REF}} \simeq 1 + \frac{\Delta K_n}{K_n} + 2 \frac{\Delta V_{th}}{V_{od}}$$

Then, some of the possible mismatch causes are:

- $K_n$ , that can varies a lot in case of wide circuits;
- $V_{od}$  that usually is set low and varies with  $V_{th}$ , whose small variation can produce large differences in the two currents;
- difference between  $V_{DS1}$  and  $V_{DS2}$ .

Assuming as maximum variations:

$$\begin{aligned} \frac{\Delta K_n}{K_n} &= \pm 5\% \\ \frac{\Delta V_{th}}{V_{GS} - V_{th}} &= \pm 10\% \end{aligned}$$

one has:

$$\frac{I_0}{I_{REF}} = 1 \pm 15\%$$

A cascaded voltage divider is connected as M2's load:

- M5 is diode connected and it is used to generate the right gate bias voltage for the gain stage.
- A resistive voltage divider made up of R2 and R4 is used to polarize the mixing stage.
- Resistors R1 and R3 are used to connect the bias net to the gain and mixing stages' gates. They also acts as high impedance for the RF and LO signals coming from outside the circuit and prevents them to enter the bias net.
- Capacitors C1 and C2 shunt possible non-DC disturbances coming from the Gilbert Cell, improving the bias isolation.

Noise issues will not be analysed within this treatise, even if it should be considered for a more complete design though. As a rule of thumb, narrow gate and low overdrive voltages should be used to lower noise contribution. (FONTE) Using a resistive voltage reference can be detrimental in case of voltage supply fluctuation, since a resistive voltage divider cannot reject current variations. However using active devices we would produce much more noise injection within the net though.

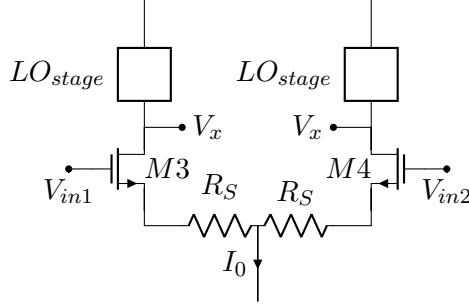


**Figure 4:** Gain stage.

**Gain stage** The gain stage (shown in figure 4) is the linear part of the mixer, it must handle without distortion and corruptions the power coming from the RF signal giving some amplification. The topology is suited for a low noise amplifying purpose (FONTE): a differential stage with source degeneration. The stage is made up of two transistors (M3 and M4) in common source configuration, polarized with current by M1, and two source degeneration resistances  $R_S$ .

The RF differential signal modulates the current flowing into each of the two transistors, that have to be polarized in saturation region. For both of them it must be ensured an high output voltage range and a quite low overdrive voltage, along with a large drain-to-source bias voltage (required to maintain the stage in saturation during the swing of the LO stage).

To have an idea on the gain that can be obtained by this stage, one can look at the stage in figure 4. Removing the degeneration resistances one has that the gate-to-gate mesh gives:

$$V_{in,1} - V_{in,2} = V_{GS3} - V_{GS4}$$

from equation 7, recalling that  $I_1 + I_2 = I_0$  and squaring:

$$(V_{in,1} - V_{in,2})^2 = \frac{2}{\beta_n} (I_0 - 2\sqrt{I_1 I_2})$$

that once inverted yields:

$$I_1 - I_2 = \sqrt{\beta_n I_0} (V_{in,1} - V_{in,2}) \sqrt{1 - \frac{\beta_n}{4I_0} (V_{in,1} - V_{in,2})^2}$$

Writing the previous equation in term of  $\Delta I = I_1 - I_2$  and  $\Delta V_{in} = V_{in,1} - V_{in,2}$  and computing the value of the slope of this characteristic, one obtains that the *maximum* differential voltage gain in equilibrium condition  $\Delta V_{in} = 0$  is given by:

$$|A_v| = \sqrt{\beta_n I_0} R_{L1} \quad (11)$$



This suggest that it is better to polarize the stage exactly with  $V_{GS1} = V_{GS2}$ . The complete expression for equation 11 also gives that the differential transconductance is a strongly non-linear function of the gate bias voltage.

As we said before there it is the possibility to have mismatch between the transistors and the loads due to circuit dimensions, temperature distribution and process tolerances. Then, looking at figure 4,  $M3 \neq M4$  and  $R_1 \neq R_2$  (where input resistance of the LO stage). It can be demonstrated that the offset output voltage due to differences in the circuit parameters and dimensions is:

$$V_{o,offset} = \Delta V_{th} + \frac{V_{GS} - V_{th}}{2} \left( - \frac{\delta R}{2R} \frac{\Delta W/L}{2W/L} \right)$$

To reduce this error a common centroid topology should be used in layout. Besides, it is important to notice that  $R_{L1}$  and  $R_{L2}$  are both the source output conductance of a common gate stage (mixing stage of the Gilbert cell) and that the actual gain for the RF stage is a current gain.

The small signal equivalent transconductance of the stage, once we added the source degeneration, (APPENDICE?) is given by:

$$G_{m,eq} = \frac{g_m}{1 + g_m R_S} \quad (12)$$

By adding  $R_S$  we lower the RF stage's current gain, however we also get a more linear behaviour reducing its dependency with respect to bias point (this fact will be demonstrated later). **LINEARITA' CON OVERDRIVE?? (RAZAVI rf PAG 193)**

The two transistors have the body contact connected to ground, this means that the threshold changes accordingly to the source to body voltage,  $V_{SB}$ :

$$V_{th} = V_{th0} + \gamma_B (\sqrt{2\phi_P + V_{SB}} - \sqrt{2\phi_P}) \quad (13)$$

This equation holds for all the transistors in the circuit, other than in current mirror.

**Mixing stage** This stage is also called *switching stage*, suggesting the way we want to drive transistors M6 to M9 (figure 5). Also this one has a differential topology, however, differently from the RF stage, we drive each pair with complementary LO signals that turn on and off cycle-by-cycle one of the two devices. A sinusoidal signal is applied to the gates (similarly one can apply a square wave), large enough to ensure the abrupt switching of the stage: when a device is on it must be in saturation (not in triode! These are actually *switch-like* transistors), while the other one must be completely off, interdicted.

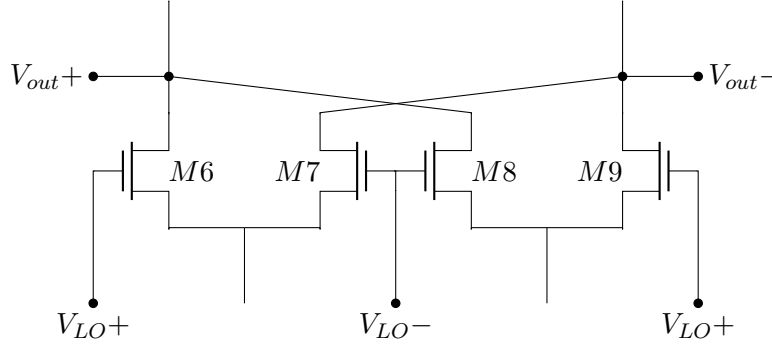


**Figure 5:** Mixing stage

A compromise is needed since:

- small amplitude of LO signals produce slower switching speed, hence part of the power is wasted as common mode signal at the output;
- too large LO signals drive the MOSFET in triode region producing spikes that corrupt the output signal with unwanted feed-through and reduces speed.

Switching speed is related to the device cut-off frequency, that for short channel devices is inversely proportional to channel length and linearly dependent to the overdrive voltage:

$$f_T \propto V_{od}/L$$

suggesting that the highest overdrive and the minimum channel length should be chosen. Again, a compromise must be found among the following solutions:

- Setting the available length ( the minimum is fixed by the used design kit);
- Selecting higher overdrive voltage one has the possibility to increase  $f_T$ , however to keep our switches in saturation and to obtain a large output swing we need to keep small this quantity;
- Widening the gate width one has faster device, but the source to bulk capacitance increases, eventually shunting the RF signal coming from the LNA stage to ground;
- Reducing the current a faster commutation is achieved, along with lower transconductance though.

Even if the switching stage is not linear it is possible to define its gain and in order to do that we analyse one single pair. We recall that the gain

LO signal modulates the stage drain current as a square wave, that can be written in term of its Fourier's series:

$$i_D(t) = I_{pk} \left( \frac{1}{2} - \frac{2}{\pi} \sum_{n=1,3,5\dots} \frac{1}{n} \sin(n\omega t) \right)$$

where only odd harmonics are present. The instantaneous gain fo the stage, related to the first harmonic is:

$$A_c|_{switch} = \frac{2}{\pi} \quad (14)$$

that is neither dependent on the bias of the stage nor on the actual device transconductance.<sup>3</sup> It is important to notice that equation 14 is exact in case of gate's square wave signals, whereas in case of sinusoidal driving the actual gain will be reduced because of the smoother variation of the drain current waveform.

**Load stage** The load stage is formed by two resistors  $R_L$  whose role is to give the stage enough gain and to set the output bias voltage through the RF drain current. They must be as matched as possible to make the differential outputs of the Gilbert cell equals.

### 2.3 Mathematical analysis: conversion gain

As already stated a mixer is a non-linear time variant system, hence a descriptive approach based on the behaviour of the cell is well suited to find the conversion gain of the cell.<sup>4</sup> The following analysis is based on the schematic in figure 6.

We suppose all the transistors in gain stage and bias in saturation, then we identify:

- $i_3$  and  $i_4$  the current through M3 and M4;
- $i_6$  and  $i_7$  the current through M6 and M7;
- $i_8$  and  $i_9$  the current through M8 and M9;
- $i_{o1}$  the current through  $R_{L1}$ ;
- $i_{o2}$  the current through  $R_{L2}$ ;

---

<sup>3</sup>It is however important to remember what stated above, regarding the intensity of the applied gate voltage, that further reduces this quantity in case of too large input signals. Moreover its better to notice that the stage introduces a loss rather than an actual gain.

<sup>4</sup>It is not possible to use neither the superposition of effect nor the Laplace transform to compute the gain due to the presence of the switching pairs.

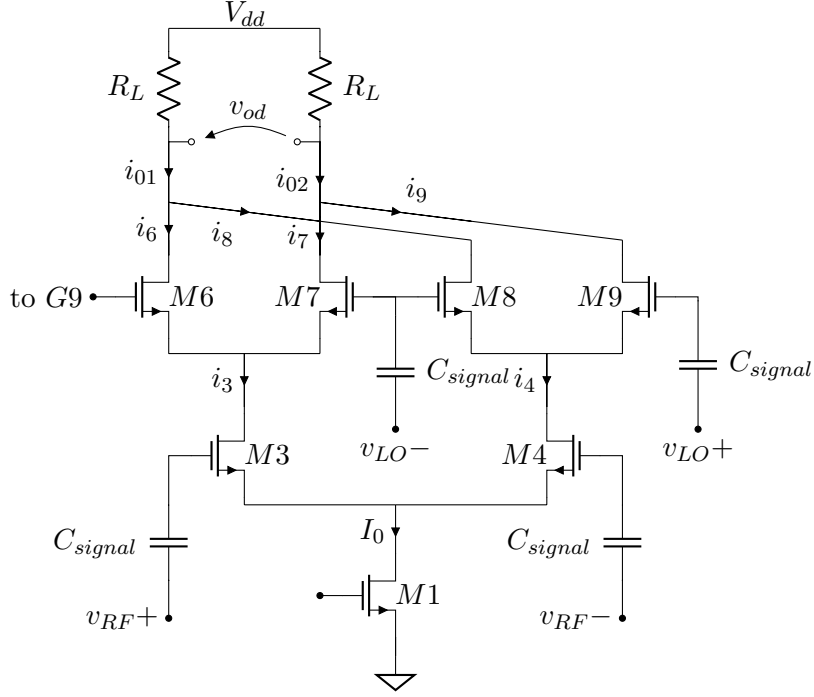


**Figure 6:** Gilbert cell, to be use as a reference for the mathematical analysis

- $I_D$  the bias current;
- $i_{od}$  the output differential bias current;
- $S(t) = \frac{1}{2} - \frac{2}{\pi} \sum_{n=1,3,5,\dots} \frac{1}{n} \sin(n\omega_{LO}t)$  is the switching function of the mixing cell (then we consider the LO stage as it was made up of ideal switches).

The differential input RF signal is given by:

$$v_{RF}(t) = \frac{V_{RF}}{2} \cos(\omega_{RF}t) \quad (15)$$

Currents flowing into the two RF stages are given by:

$$i_3(t) = I_D + i_d(t) \quad (16)$$

$$i_4(t) = I_D - i_d(t) \quad (17)$$

where, from equation 12, the  $i_d$  current is a small signal variation given by:

$$\begin{aligned} i_d(t) &= I_{RF} \cos(\omega_{RF}t) \\ &= G_{m3,4} \frac{V_{RF}}{2} \cos(\omega_{RF}t) \end{aligned} \quad (18)$$

It is now possible to define the current flowing into the switching stage recalling that they are discontinuous functions modulated by the switching function  $S(t)$ :

$$i_6(t) = [I_D + i_d(t)]S(t) \quad (19)$$

$$i_7(t) = [I_D + i_d(t)]S(t - T_{LO}/2) \quad (20)$$

and

$$i_8(t) = [I_D - i_d(t)]S(t - T_{LO}/2) \quad (21)$$

$$i_9(t) = [I_D - i_d(t)]S(t) \quad (22)$$

because M6 and M9 share the same LO signal; the same holds for M7 and M8. Hence the current through  $R_{L1}$  and  $R_{L2}$  is given by:

$$\begin{aligned} i_{o1}(t) &= I_6(t) + I_8(t) \\ &= [I_D + i_d(t)]S(t) + [I_D - i_d(t)]S(t - T_{LO}/2) \end{aligned} \quad (23)$$

and

$$\begin{aligned} i_{o2}(t) &= I_7(t) + I_9(t) \\ &= [I_D + i_d(t)]S(t - T_{LO}/2) + [I_D - i_d(t)]S(t) \end{aligned} \quad (24)$$

Therefore, the output differential current is:

$$\begin{aligned} i_{od}(t) &= I_{o1}(t) - I_{o2}(t) \\ &= 2i_d(t)S(t) - 2i_d(t)S(t - T_{LO}/2) \end{aligned} \quad (25)$$

Noticing that:

$$\begin{aligned} S(t - T_{LO}/2) &= \frac{1}{2} - \frac{2}{\pi} \sum_{n=1,3,5,\dots} \frac{1}{n} \sin(n\omega_{LO}t - T_{LO}/2) \\ &= \frac{1}{2} + \frac{2}{\pi} \sum_{n=1,3,5,\dots} \frac{1}{n} \sin(n\omega_{LO}t) \\ &= 1 - \frac{1}{2} + \frac{2}{\pi} \sum_{n=1,3,5,\dots} \frac{1}{n} \sin(n\omega_{LO}t) \\ &= 1 - S(t) \end{aligned} \quad (26)$$

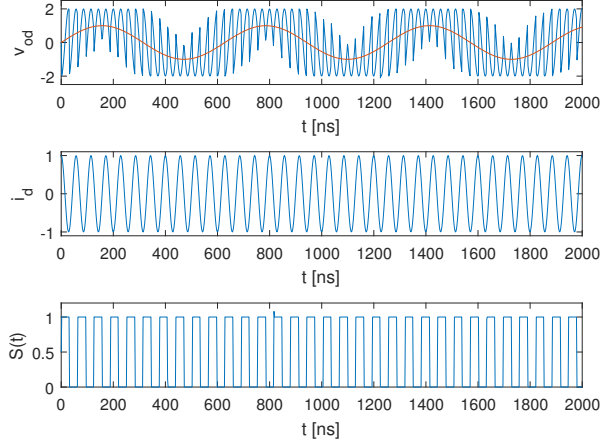


**Figure 7:** Ideal signal modulation within Gilbert cell.

and substituting equation 26 in 25 we get:<sup>5</sup>

$$\begin{aligned}
 i_{od}(t) &= -\frac{8i_d(t)}{\pi} \sum_{n=1,3,5\dots} \frac{1}{n} \sin(n\omega_{LO}t) \\
 &= -\frac{8I_{RF}}{\pi} \cos(\omega_{RF}t) \sum_{n=1,3,5\dots} \frac{1}{n} \sin(n\omega_{LO}t) \\
 &= -\frac{8I_{RF}}{\pi} \sum_{n=1,3,5\dots} \frac{1}{n} \cos(\omega_{RF}t) \sin(n\omega_{LO}t) \\
 &= -\frac{8I_{RF}}{\pi} \sum_{n=1,3,5\dots} \frac{1}{2n} \left\{ \sin[(\omega_{RF} + n\omega_{LO})t] + \sin[(\omega_{RF} - n\omega_{LO})t] \right\}
 \end{aligned} \tag{27}$$

The full ideal output differential signal is shown in figure 7. Considering only the fundamental tone of the LO signal (other frequency terms are out-of-band with respect to IF) and multiplying by  $R_L = R_{L1} = R_{L2}$  one finds that the differential output voltage is given by:

$$\begin{aligned}
 v_{od}(t) &= -\frac{4I_{RF}R_L}{\pi} \{ \sin[(\omega_{RF} + \omega_{LO})t] + \sin[(\omega_{RF} - \omega_{LO})t] \} \\
 &= -\frac{4I_{RF}R_L}{\pi} [\sin(\omega_{HF}t) + \sin(\omega_{IF}t)]
 \end{aligned} \tag{28}$$

then, referring to the IF component:

$$\begin{aligned}
 v_{od,IF}(t) &= -\frac{4I_{RF}R_L}{\pi} \sin(\omega_{IF}t) \\
 &= -\frac{2G_{m3,4}R_LV_{RF}}{\pi} \sin(\omega_{IF}t)
 \end{aligned} \tag{29}$$

---

<sup>5</sup>  $\cos(x)\sin(y) = \frac{1}{2}\sin(x+y) + \frac{1}{2}\sin(x-y)$

that, considering the IF and RF *rms* values eventually yields the Gilbert cell mixer conversion gain:

$$A_{vC} = \frac{2}{\pi} \frac{R_L}{\frac{1}{g_{m3,4}} + R_S} \quad (30)$$

It is now possible to highlight that:

- in first approximation the conversion gain does not depends on the amplitude of the LO signal;
- both LO and RF components are rejected at the output;
- it is possible to keep only the IF component by filter out the HF signal;
- the degeneration resistance  $R_S$  improve the stage's linearity. In fact, if properly chosen, one has:  $A_{vC}|_{g_{m3,4} \ll R_S} \simeq \frac{2}{\pi} \frac{R_L}{R_S}$ . Besides to linearity, the conversion gain is less sensitive with respect to the RF stage bias point;
- no informations about frequency behaviour appear with this kind of analysis.

### 3 Design by hand of a down-converting Gilbert cell

#### 3.1 Design specifications

The design specifications follow:

- The use technology is the AMI  $0.6\mu\text{m}$  by MOSIS. **No constraints regarding maximum gate width are considered. This technology is nowadays old-fashioned, hence this project has only didactic purposes.** The Cadence Design Environment will be used to carry on the project;
- the supply voltage is  $V_{DD}=5\text{V}$ ;
- we are design a down-conversion mixer. The analysis will be carried on considering two monochromatic signals  $f_{RF}=110\text{ MHz}$  and  $f_{LO}=100\text{ MHz}$ , producing a wanted baseband signal at  $f_{IF}=10\text{ MHz}$  (the HF component is considered as filtered out);
- all the transistors should work in saturation;
- the conversion gain is chosen accordingly to the previous specification equal to  $G_{VC}=15\text{dB}_{20}$ .

The most important parameters used in the design are reported in the following table: <sup>6</sup>

**Table 1**

| Parameter Name | Value | Unit                      |
|----------------|-------|---------------------------|
| $A_{vC}$       | 5.6   |                           |
| $V_{DD}$       | 5     | V                         |
| $I_0$          | 5     | mA                        |
| $V_{th0}$      | 0.709 | V                         |
| $K_n$          | 116   | $\mu\text{A}/\text{V}^2$  |
| $I_{dss}$      | 466   | $\mu\text{A}/\mu\text{m}$ |
| $\phi_P$       | 0.7   | V                         |
| $\gamma_B$     | 0.5   | V                         |
| $L_{min}$      | 0.6   | $\mu\text{m}$             |

It is necessary to notice that the following calculation is carried on considering the easiest between the physic-based models for a MOSFET, i.e. the level 1 model and its aim is to make the reader to understand the

<sup>6</sup>MOSFET's parameters are intended at  $T=27^\circ\text{C}$



design choices that follow in the next section. Moreover, the used model relies on a level 3 model, that takes count of short channel effects (we are using sub-micrometric devices) and non-ideality such as the carrier velocity saturation.

### 3.2 Gilbert cell design flow

**Current mirror bias** Both M1 and M2 must be in saturation. We choose the same current to flow in the weak and strong branches in order to have equal structures (this aids the circuit symmetry and matching, allowing us to use interdigitated structure). We impose:

$$I_{D1} = I_{D2} = I_0 = 5mA \quad (31)$$

$$V_{od1} = V_{od2} = 0.4V \quad (32)$$

$$L_1 = 3L_{min} = 1.8\mu m \quad (33)$$

The current magnitude is chosen thinking about the mixer used in a transmitter receiving chain, after an hypothetical power stage. The overdrive voltage's value is chose in order to keep turned on the stage even with strong fluctuation of the drain node. However, to have the same current mirrored we must have:

$$V_{GS1} = V_{GS2}$$

$$V_{DS1} = V_{DS2}$$

$$W_1 = W_2$$

suggesting that this kind of current source can work properly only with small signal variation coming from the RF stage. Now, by using 7, neglecting channel modulation effects and inverting:

$$W_1 = \frac{2I_0}{K_n V_{od1}^2} L_1 = 969.8\mu m \quad (34)$$

Both M1 and M2 are not affected by body effect, then:

$$V_{th1} = V_{th2} = V_{th0}$$

hence:

$$V_{GS2} = V_{DS2} = V_{th0} + \sqrt{\frac{2I_0 L_1}{K_n W_1}} = 1.1V \quad (35)$$

The design for the voltage reference bias net is reported in section 4.

**Load stage and gain choice** As previously stated we chose  $A_{vC}=4$ . Since the whole differential structure must be symmetrical, current  $I_0$  is evenly split into M3 and M4: this is the same current flowing also into the two loads. In order to give the LO stage **enough output swing** we impose one third of the supply voltage must drop on the load. Therefore, we can calculate the load resistance's value:

$$R_L = \frac{\frac{2}{3}V_{DD}}{I_0/2} = 1.33k\Omega \quad (36)$$

**Gain stage bias** The design of the RF bias begins with the choice of its transconductance, fixed by  $A_{vC}$ ,  $R_L$  and  $R_S$ . We consider M3 and M4 equal and in saturation. The gate length for this stage is set

$$L_3 = L_4 = 3L_{min} = 1.8\mu m \quad (37)$$

The degeneration resistance's value is chosen equal to  $10\Omega$ , hence:

$$V_{R_S} = \frac{R_S}{I_0/2} = 25mV \quad (38)$$

Now, by inverting equation 30:

$$g_{m3} = \frac{\pi}{2} \frac{1}{\frac{R_L}{A_{vC}} - R_S} = 6.9mS \quad (39)$$

We notice that we have many variables that are involved and that directly affect the design feasibility:

- high values of  $R_S$  decrease the RF stage transconductance, requiring large transistors with low overdrives. Low values give instead more transconductance and linearity reducing the output dynamic though;
- increasing the conversion gain we have the same effects reported before, however mixing signals is a strongly inefficient operation, then we cannot reduce too much this quantity;
- the choice of the load is important to fix the output dynamic and must be chosen carefully.

By inverting equation 11:

$$W_3 = g_{m3}^2 \frac{2L_3}{K_n I_0} = 148.5\mu m \quad (40)$$

We have body effect due to the source to body voltage, shared by M3 and M4:

$$V_{SB3} = V_{DS1} + V_{R_S} \quad (41)$$

then, from equation 13:

$$V_{th3} = V_{th0} + \gamma_B(\sqrt{2\phi_P + V_{SB3}} - \sqrt{2\phi_P}) = 0.957V \quad (42)$$

from which it comes that:

$$V_{od3} = \sqrt{\frac{I_0}{K_n W_3/L_3}} = 0.723V \quad (43)$$

$$V_{GS3} = V_{th3} + V_{od3} = 1.731V \quad (44)$$

Unfortunately the value of the overdrive voltage looks large (**FORTE**), requiring us to fix  $V_{DS3,4}$  high enough to avoid the stage to be turned off by LO's output swing. We impose to have half the supply voltage to drop on the gain stage and current mirror, having:

$$V_{DS3} = \frac{1}{2}V_{DD} - V_{DS2} = 1.4V \quad (45)$$

To ensure saturation of M3 and M2 we set:

$$V_{G3} = V_{GS3} + V_{RS} + V_{DS1} = 2.805V \quad (46)$$

**Mixing stage bias** Also in this case we require transistors from M6 to M9 to be in saturation (they are equal and biased the same way). We reduce as much as possible the overdrive voltage: in this way the stage is kept nearby the threshold fostering a the commutation of the switches. Having small overdrives we produce large transistors then, to limit this we set:

$$L_6 = L_{min} \quad (47)$$

$$V_{od6} = 150mV \quad (48)$$

By using 7 and taking in count the body effect we get:

$$W_6 = 1.1mm \quad (49)$$

$$V_{SB6} = V_{DS1} + V_{RS} + V_{DS2} \quad (50)$$

$$V_{th6} = 1.18V \quad (51)$$

This result does not consider short channel effects, that produces a different threshold dependency on source to bulk voltage. However, considering ideal behaviour we have that the M6 to M9's bias gate voltage is:

$$V_{GS6} = 1.326V \quad (52)$$

$$V_{G6} = V_{GS6} + V_{DS1} + V_{RS} + V_{DS2} = 3.855V \quad (53)$$

## 4 Design by simulation

### 4.1 Gilbert Cell design

After simulating the design made with Level 1 model, simulation results proven to be not enough accurate to have a correctly behaving circuit. For this reason a new design was carried on taking advantage of the simulated trans-characteristic of each stage.

In literature (**FORTE**) an optimum value for transistors width in mixers is proposed:<sup>7</sup>

$$W_{opt} = \frac{1}{3\omega LC_{ox}R_g} \quad (54)$$

where  $\omega$  is the stage's working frequency (i.e.  $f_{LO}$  or  $f_{RF}$ ),  $L$  is the channel length,  $C_{ox}$  is the MOSFETS's total oxide capacitance and  $R_g$  the generator output resistance (we set this value equal to  $50\Omega$ ). Values coming from this formula are actually too large ( $\geq 1mm$ ), therefore we chose to pursue another approach to begin the design.

The starting specification was to maximize  $g_{m3}$  of the input RF stage, with some reasonable hypotheses on transistor dimensions and power consumption.

$$\begin{aligned} L &= 3L_{min} = 1.8\mu m \\ 50\mu m &\leq W_3 \leq 500\mu m \\ I_0 &\approx 5mA \end{aligned}$$

Further, suppositions on bias voltages were made. For example, a voltage equal to  $\frac{3}{5} \cdot V_{dd}$  was supposed to drop between the RF stage's drain and ground, equally divided between M1 and M3 (neglecting the very small voltage drop on  $R_S$ ).

$$V_{SB3} = V_{DS1} = V_{DS3} = 1.5V$$

This way allows us to take into account the body effect on threshold voltage of transistor M3. Then we plotted the current and transconductance of the transistor as a function of  $V_{GS}$  and  $V_{DS}$ , that are shown in pictures 8a and 8b.

---

<sup>7</sup>More generally, this gives a compromise between power dissipation and noise in LNA.

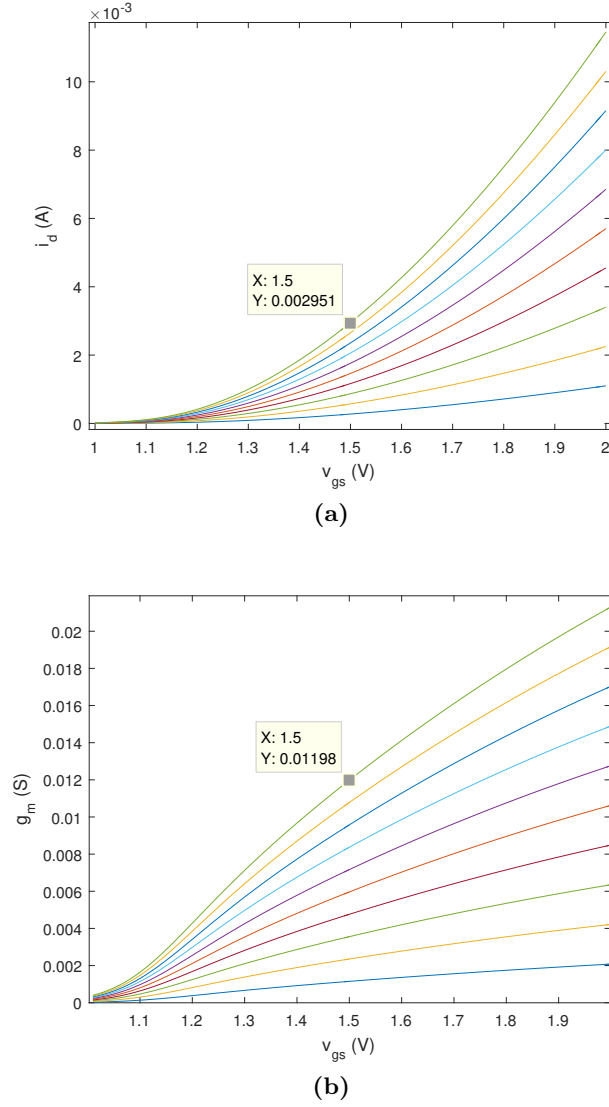


**Figure 8:** a) Drain current versus gate-source voltage of the RF stage, with  $W$  varying from  $50\mu m$  to  $500\mu m$ . b) Transconductance versus gate-source voltage of the RF stage, with  $W$  varying from  $50\mu m$  to  $500\mu m$ .

The largest width  $W_3 = 500\mu m$  (the green curve) was chosen, along with  $V_{GS3} = 1.5V$ , accordingly to the current and transconductance's value, eventually taking the highest values:

$$g_{m3} = 11.9mS$$

$$\frac{I_0}{2} = 2.9mA$$

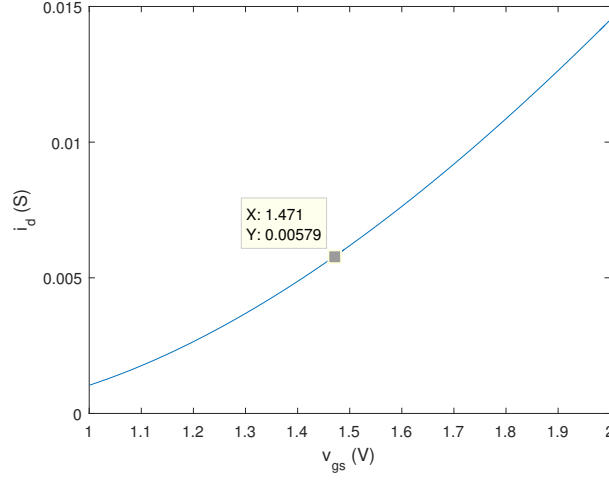


**Figure 9:** Drain current versus gate-source voltage of the bias transistor M1, with  $W=373\mu m$

We moved then to current sink design, M1 and M2. Given the data:

$$\begin{aligned} V_{R_S} &= 2.9mA * 10\Omega = 29mV \\ V_{DS1} &= 1.5V - V_{R_S} = 1.471V \\ V_{GS1} &= 1.471V \end{aligned}$$

This set of values leads to a width equal to  $W_1 = 373\mu m$  in order to have  $I_0 = 2 \cdot 2.9mA = 5.8mA$  (figure 9).

Finally the LO stage was designed, along with the load resistance  $R_L$  starting from the wanted conversion gain, lowered to  $A_v = 4$  with respect to what we decided in the previous section. Given the analytic expression of voltage conversion gain 30 (**FORTE**):

$$A_v \approx \frac{2}{\pi} \left( \frac{R_L}{R_S + \frac{1}{g_{m3}}} \right) = 4$$

The value of  $R_L$  is then determined

$$R_L = A_v \cdot \left( \frac{\pi}{2} \cdot \frac{1}{g_{m3}} + R_S \right) = 577\Omega \quad (55)$$

The drain-to-source voltage of the LO stage,  $V_{DS6}$ , can be thus evaluated as follows:

$$\begin{aligned} V_{SB6} &= V_{DS1} + V_{R_S} + V_{DS3} \\ &= 1.47V + 0.029V + 1.5V = 3V \end{aligned}$$

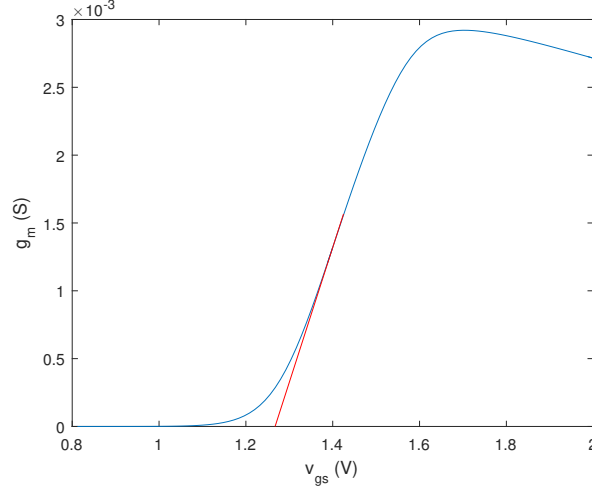


**Figure 10:** Extrapolation of M6 threshold voltage from transconductance versus the  $V_{GS}$  curve. The threshold happens to be at  $1.27V$ .

and

$$V_{RL} = 2.9mA \cdot 577\Omega = 1.673V$$

$$V_{DS6} = V_{dd} - V_{RL} - V_{SB6} = 327mV$$

The LO gate bias voltages must be slightly above the threshold, in order to let the transistors turn on and off with small LO signal variations, deviating rapidly current coming from the RF stage. To accomplish this, the transistor's threshold was extracted from simulation, using the  $g_m$  graph as a function of  $V_{GS}$  (figure 10). Having  $V_{th6} = 1.27V$ , a very small overdrive of  $\Delta V_6 = 60mV$  was chosen, for the reason reported before, and to assure the stage is not working in triode region. This leads to:

$$V_{GS6} = V_{th6} + \Delta V_6 = 1.33V$$

Once fixed the node's voltages and the current flowing in the transistor ( $2.9mA$ , due to the fact that only two transistors of LO stage conduct simultaneously), transistor width  $W_6$  was swept to fulfil precisely this biasing. The followed procedure is the same displayed in figure ?? and the resulting found dimensions are:

$$W_6 = 170.3\mu m$$

$$L = L_{min} = 0.6\mu m$$

Only for this stage the minimum channel length was taken, in order to keep small these transistors regardless overdrive small value.

## 4.2 Biasing network design

From the previous section, the bias network specifications required by current sink, RF and LO stage are suddenly imposed:

$$V_{G1} = 1.471V$$

$$V_{G3} = 3V$$

$$V_{G6} = 4.33V$$

The bias network circuit employed is visible in **figure**.

The mirroring ratio for the current sink transistor M1 was chosen to be 1 as chosen in section 3. With a transistor length  $L_2 = 1.8\mu m$ , and being  $V_{GS2} = V_{DS2} = 1.471V$  imposed,  $W_2$  has been trimmed in the simulator to sink a current equal to  $I_0 = 5.8mA$ , resulting in:

$$W_2 = 373\mu m$$

In the same way transistor M5 width was set, in order to have a gate voltage  $V_{G5} = 3V$  when stacked above M2:

$$W_5 = 130.45\mu m$$

$$L_5 = 0.6\mu m$$

Minimum length was taken in this case to reduce the transistor's size. The sum of  $R_2$  and  $R_4$  must be such that with total current of  $5.8mA$ , the voltage drop across them is such that  $V_{G5} = 3V$ :

$$R_2 + R_4 = \frac{V_{dd} - V_{G5}}{I_0} = 344\Omega$$

The partition between them must give a bias voltage to LO stage of  $4.33V$ . This brings to

$$R_2 = 229\Omega$$

$$R_4 = 115\Omega$$

Resistors  $R_1$  and  $R_3$  were chosen to be large enough to isolate biasing network from RF and LO signals respectively, and form a low pass filter along with capacitors  $C_1$  and  $C_2$ . Resistors were thus chosen of the order of some  $k\Omega$ .

$$R_1 = R_3 = 30k\Omega$$

From here, the minimum capacitance to filter out LO signal can be evaluated in order to have a pole at least one decade before working frequency. The



output resistance of M5 has been considered negligible with respect to  $R_1$  and  $R_3$ , leading to an equivalent resistance for the low pass filter equal to:

$$R_{eq} = R_1 // R_3 // R_2 // R_4 = 76.4\Omega$$

from which the resulting capacitance:

$$C_1 \geq 10 \cdot \frac{1}{2\pi \cdot R_{eq} \cdot f_{lo}} = 20.8pF \quad (56)$$

$C_1 = C_2$  was chosen for simplicity. Finally a CAD optimization over them was carried on to maximize the gain and minimizing the capacitors' dimensions, leading to the final chosen value of:

$$C_1 = C_2 = 25pF \quad (57)$$

## 5 Layout of the Gilbert Cell

The overall layout was carried on in place with a view to:

- reducing technology gradients using common centroid, interdigitated or multi-finger structures;
- placing components all in the same direction for a uniform error affection;
- reducing border effects with dummy elements;
- minimizing encroachment errors with same-length transistor fingers;
- limiting substrate noise with guard rings;
- avoiding connections which could lead to crosstalk;
- minimizing metal changes in the routing process;
- aiming a compact structure.

### 5.1 Differential RF stage

A careful attention has been paid to the layout of differential pairs like the one of RF stage. Since it's desirable to have the most symmetric input stage a common centroid configuration has been employed, following a structure sketched as in figure 11.

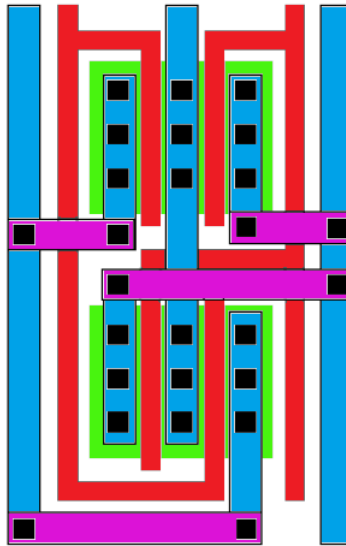


**Figure 11:** Common centroid structure used for differential RF stage

This minimizes errors due to process gradients within the planar structure. Dummy elements were also placed next to the four transistors at the edges to guarantee a uniform dopant concentration of the inner transistors.

Dummy MOSFETs' drain and source are tied together and then short circuited to source. The transistor length of the differential pair has been divided to form multi-finger transistors, such that the whole structure results as square and compact as possible. This was intended again for the purpose of reducing gradients and with a glance forward to the overall mixer layout's compactness. The final layout of differential RF pair is shown in figure 12.

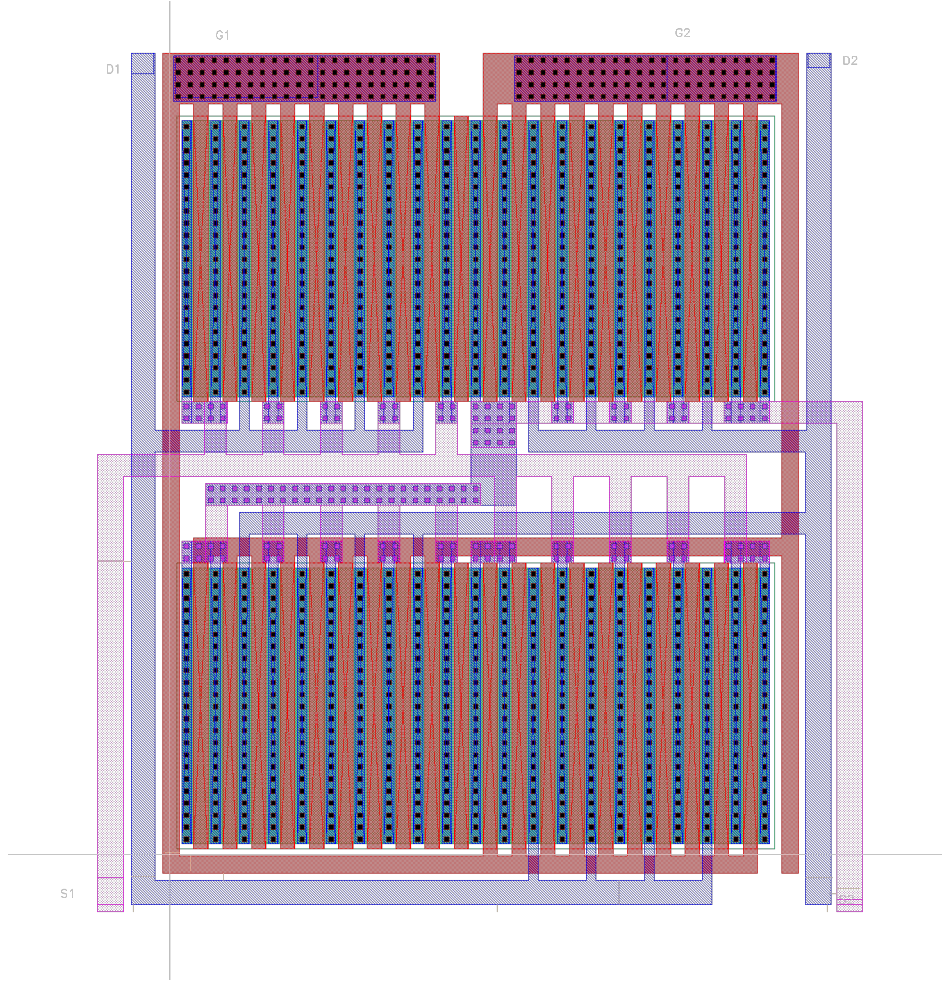


**Figure 12:** Complete layout of RF differential transistor

## 5.2 Differential LO stages

The two differential LO stages have been designed trying to prevent the same mismatch causes seen for the RF stage. Two common centroid structure were drawn at first. Being the transistor wide, multi-finger structure was employed also here to have an almost-square layout along with dummy elements. Attention has been paid in so that the two LO pairs could be easily stack above the RF stage with the same width. Secondly, we opted for a merging of the two common centroid LO layouts in a more compact tiled layout. The gate disposal simplifies the access to these nets from the signal capacitors in the global layout. Final LO layout is shown in figure 13 .

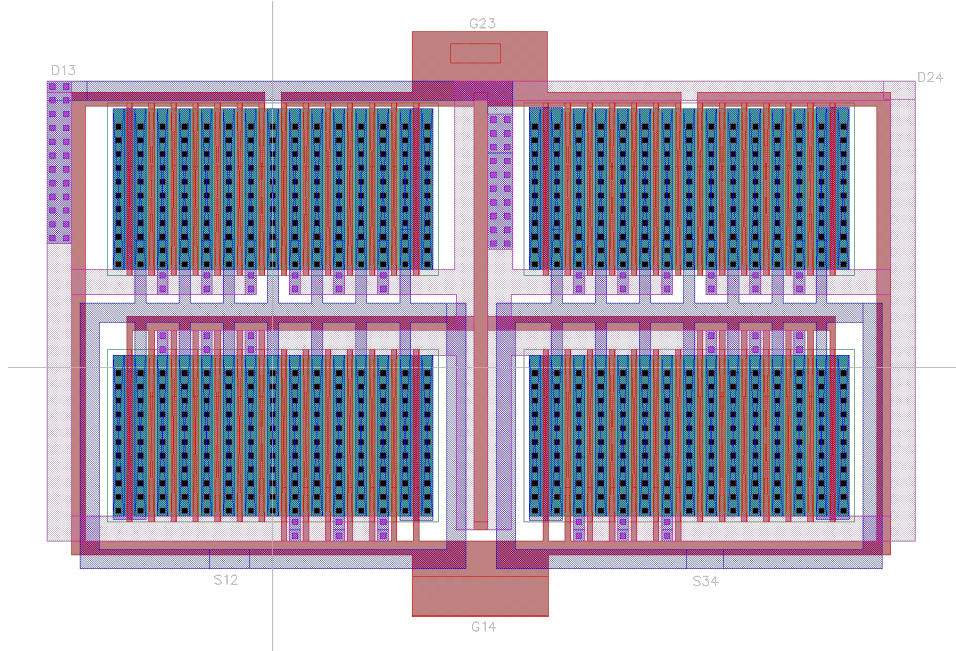


**Figure 13:** Complete layout of LO differential stages

## 5.3 Current mirror and diode connected transistor

Current mirror employs an interdigitated structure similar to the one visible in **figure**.

Since fingers are all the same size the current ratio is independent from encroachment width. Dummy transistors was included to reduce border effects, and source connections on both top and bottom sides have been added for a small source resistance. The weak branch transistor's drain has been tied together to the gate with an array of contacts. The final layout for current mirror is visible in 14.



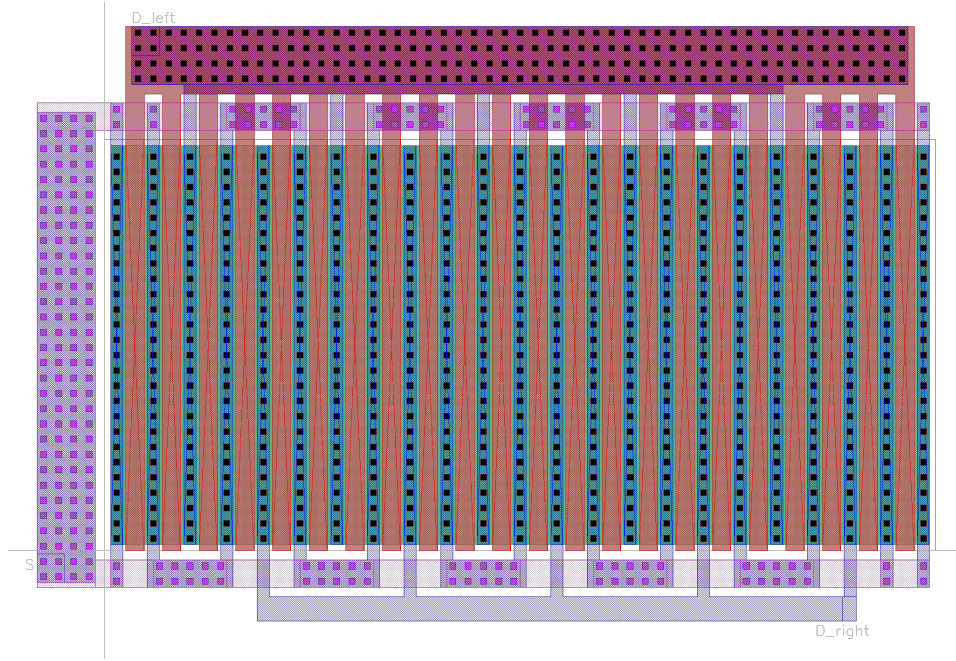


**Figure 14:** Complete layout of current mirror

Concerning the diode-connected transistor M5, interdigitated structure was implemented. Dummy transistors are placed aside whereas an array of contacts to minimize series resistance between gate and drain has been added. Final layouts and highlighted nets are visible in figure 15.

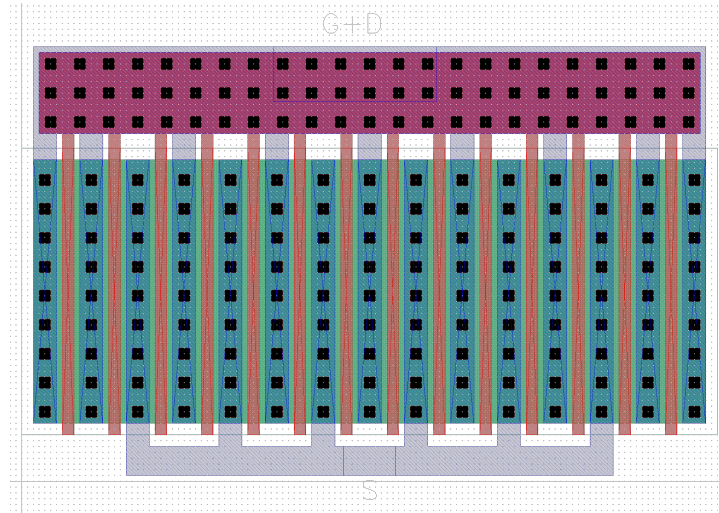


**Figure 15:** Complete layout of M5 transistor

## 5.4 Capacitors

**Bias capacitors** Bias capacitors have been designed using two configurations of common centroid layout. A simplified version of the layout structure implemented is drawn in figure 16.

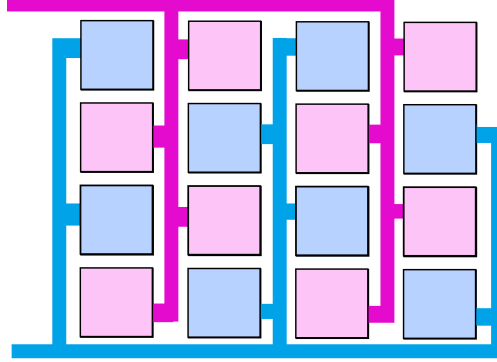


**Figure 16:** Bias capacitors layout structure

Even if no exact ratio between the two capacitors is needed, a modular geometry, made by equal squares, was used. This minimizes undercut effects, and the square shape reduces border errors. In order to reduce the area, capacitor units were designed using poly1 and poly2 (elec) layers, which give the maximum capacitance per unit area available with this technology kit. A dummy capacitor frame was placed around to minimize border effect. All the capacitors lie above an n-well, whose purpose is to minimize fringing field leakage. This n-well is tied to  $V_{DD}$  potential. The final layout with highlighted nets is visible in figure 17.

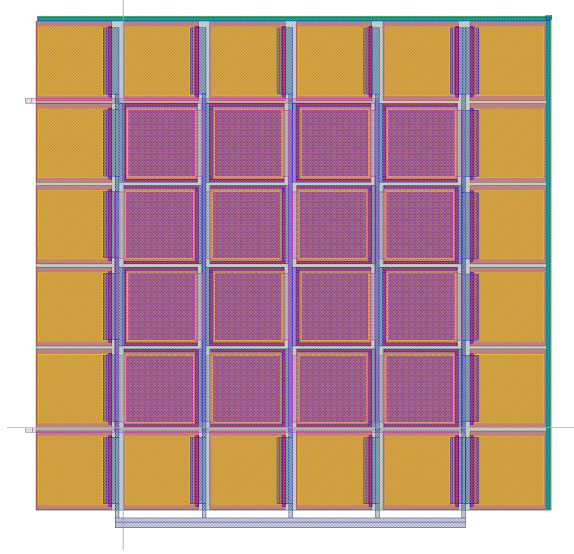


**Figure 17:** Full layout of  $C_{bias}$  capacitors

**Signal capacitors** Since these capacitors resulted to be very space demanding due to capacitance value, a multi-layer capacitor was tried to be built alternating poly and metal layers. Unfortunately this idea was soon abandoned due to the *rule 11.6 of SCMOS rules*, which does not allow unrelated metal layer over poly2. The most practical solution proven to be using poly1-to-poly2 capacitance in a common centroid structure. This time matching is more important with respect to bias capacitors, because we want signal coming to the differential stages pass through strongly symmetrical paths. A simplified version of the common centroid structure implemented is shown in figure 18.

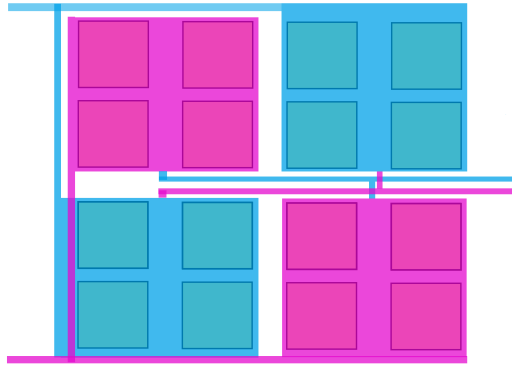


**Figure 18:** Common centroid structure of the signal capacitors

Since this is a high frequency path to reduce series resistance and inductance, metal plates with contacts were placed all over the square unit capacitors. Dummy short circuited elements were positioned all around the capacitor as well. An additional n-well connected to  $V_{DD}$  surrounds the capacitor to reduce fringing field leakage. The overall capacitance layout with highlighted nets is visible in figure 19.

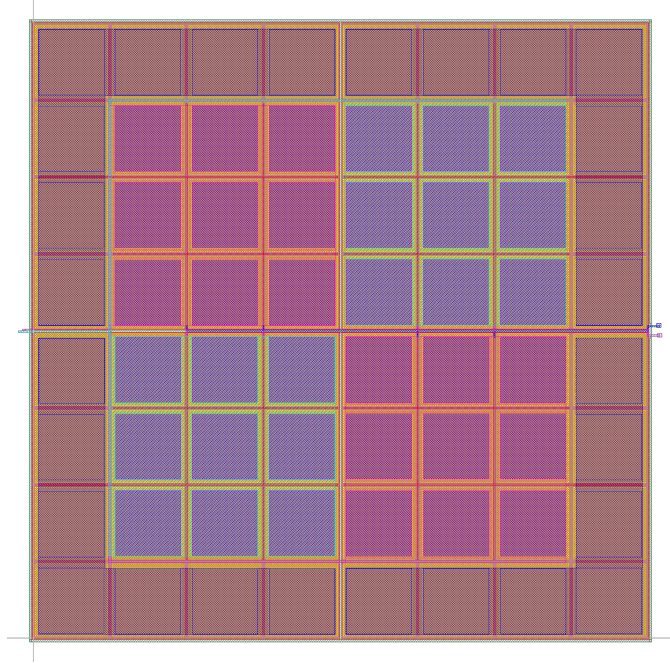


**Figure 19:** Full layout of  $C_{signal}$  capacitors

## 5.5 Resistors

Two kinds of resistors have been implemented in this layout, both of them are described in the following paragraphs.

**N-well resistors** Resistors fabricated in n-well have worse tolerance, but an higher sheet resistance. That's the way this kind of resistor was chosen to implement biasing resistors  $R_1$  and  $R_3$ , which are, as a matter of fact, very large in absolute value, but their tolerance is not too important. We can thus have smaller layout adopting n-well layout. Resistors were split in modular structures with the common centroid fashion to reduce differences between  $R_1$  and  $R_3$ . Due to the fact that this resistors are very close to the mixing stage, a guard ring connected to ground has been included to prevent substrate noise being injected through the biasing network. The final layout obtained for  $R_1$  and  $R_3$  resistor is visible in 20.



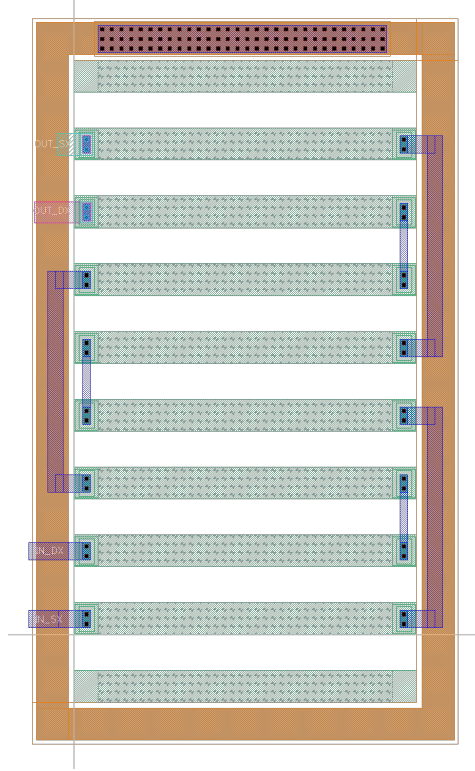


**Figure 20:** Layout of  $R_1$  and  $R_3$  resistors

**Poly silicon resistors** Since other resistors are smaller than  $R_1$  and  $R_3$ , poly has been employed to build them, taking advantage of their higher precision but smaller sheet resistance. All of them were drawn in common centroid structure, except for  $R_4$  (due to its small value), and dummy elements on both sides were always used. Final layouts for these resistors are shown in 21a,21b,21c,21d. Dimensions are not in scale.

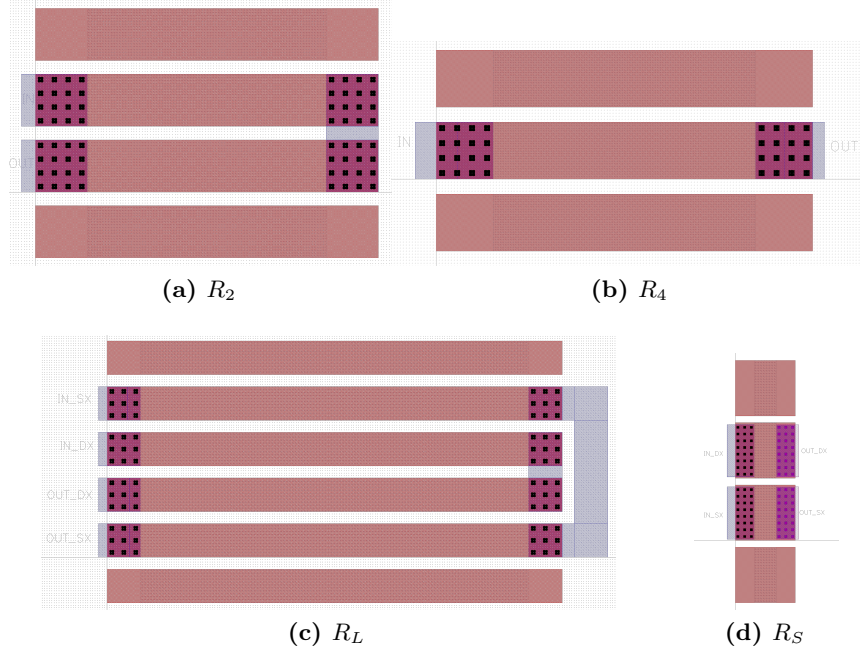


**Figure 21:** Poly resistors layout

## 5.6 Putting together the layout

The layout has been organized in order to minimize the occupied surface area. The final configuration can be seen in figure 22.

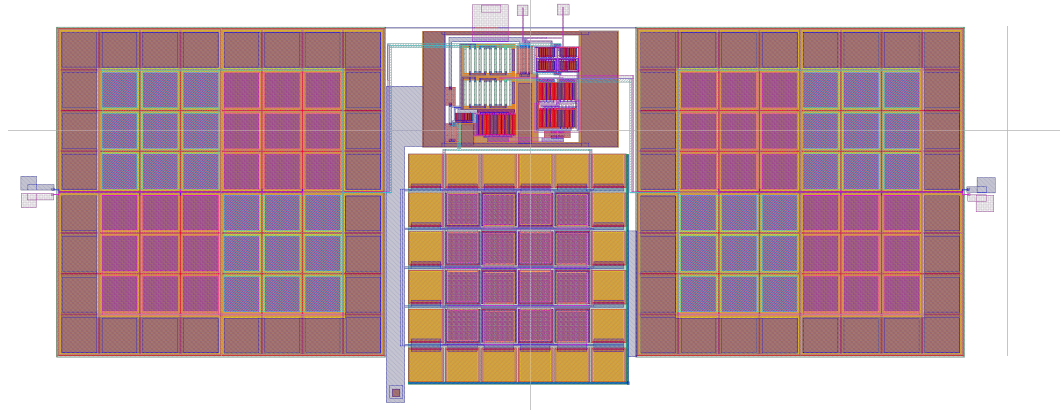


**Figure 22:** Layout of the complete Gilbert balanced mixer

Components have been placed to shorten interconnections, emphasize symmetries for matching and to make paths as equal as possible for high frequency signals. Body contacts were placed all around the circuit where possible, and then connected to ground, in order to capture free charges in the

substrate reducing noise. A close up vision of the complete layout, without capacitors, is visible in figure 23.

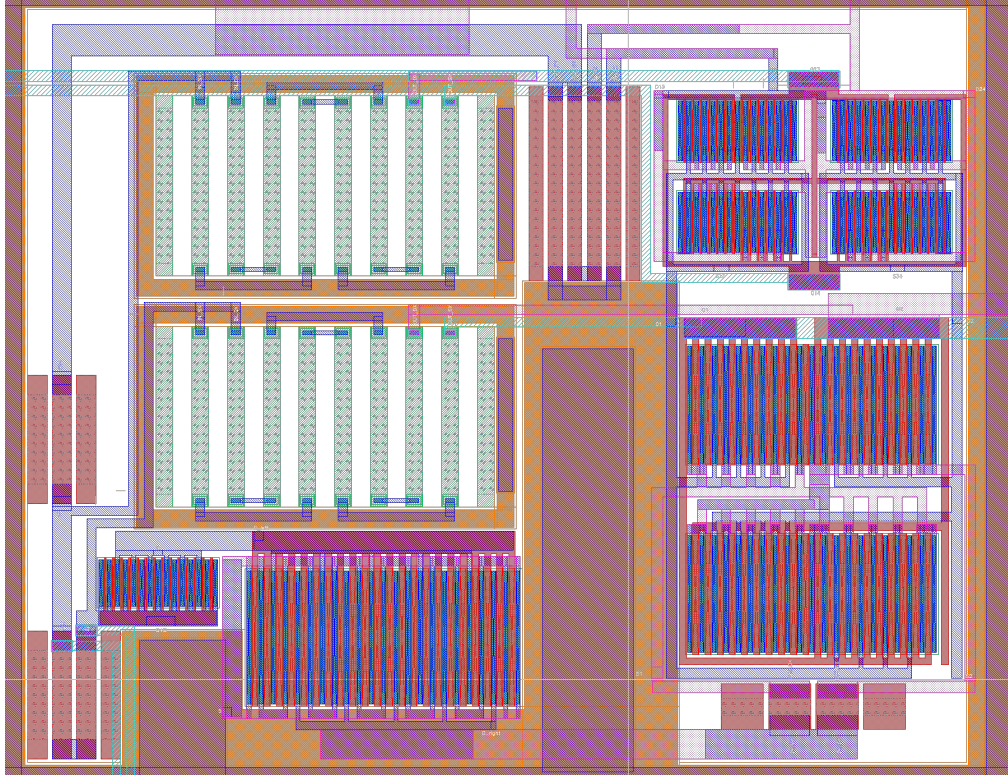


**Figure 23:** Close up of the complete layout

The whole occupied area is approximately  $0.7mm \times 1.8mm$  and it's mainly due to size of the signal capacitors. Such a big area can be also justified with the fact that the used technology is not the right one for this kind of RF design, and it was carried on mainly with the scope of learning how to layout a circuit.

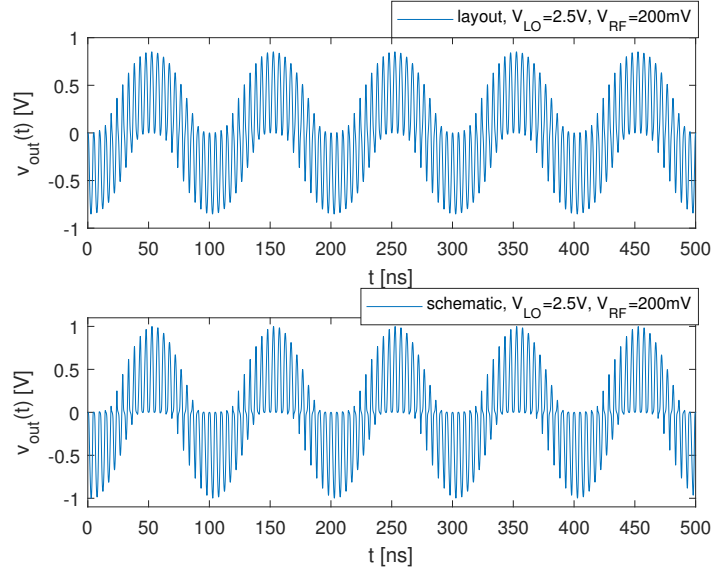


**Figure 24:** Time domain waveforms: double balanced differential output with  $V_{RF}=200\text{mV}$ ,  $f_{RF}=110\text{MHz}$ ,  $V_{RF}=1.23\text{mV}$ ,  $f_{LO}=100\text{MHz}$ .

## 6 Simulation vs schematic comparison

### 6.1 Simulation setup

Last step was to characterize the layout and evaluate its behaviour in comparison with the schematic. The carried on analysis are the following:

- Time domain mixed signal and spectral components;
- Oscillator amplitude to maximize output component;
- Conversion gain and 1dB compression point;
- Single tone  $\text{IIP}_3$ ;
- Two tone  $\text{IIP}_3$ ;
- Bandwidth and CMRR of RF stage (output node filtering of output signal, current mixing);
- Static power dissipation;

All the analysis were developed using monochromatic signals at frequencies 100MHz for LO, 110MHz for RF, and considering the mixer working in down-conversion (10MHz IF frequency).

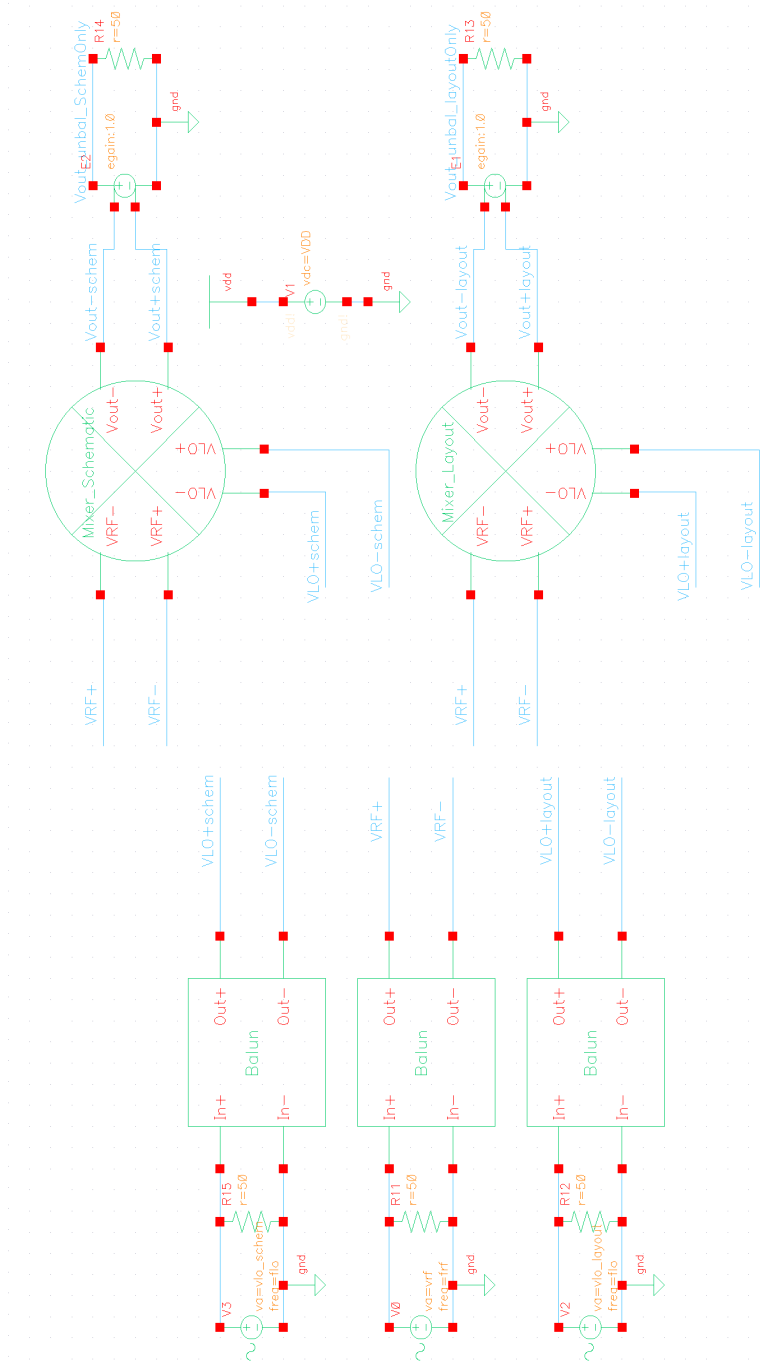


**Figure 25:** Simulation set-up.

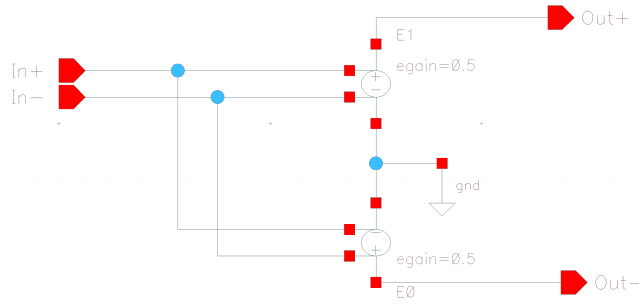
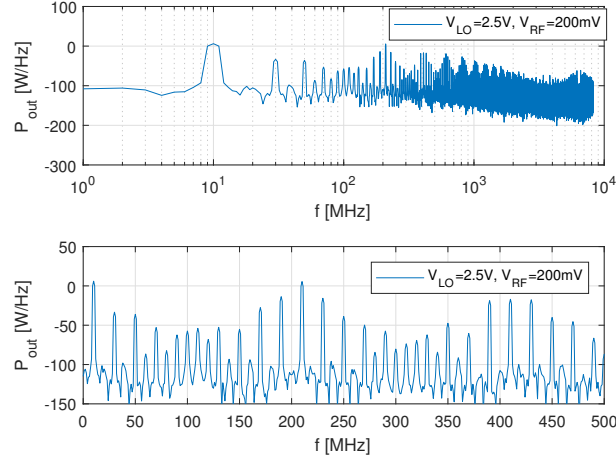


**Figure 26:** Balun schematic.

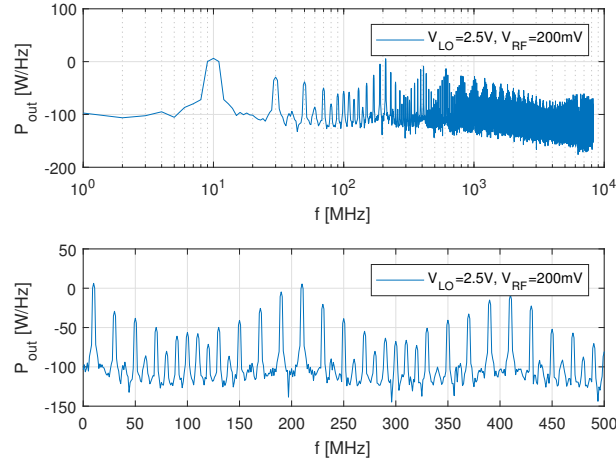
To compare schematic and layout we used the set-up proposed in figure 25, that includes:

- The symbols related to mixer's schematic and layout under test.
- Input AC signals generators. Those elements are connected to ideal baluns (figure 26) in order to simulate a perfect  $50\ \Omega$  impedance matching condition, producing differential inputs also. Two LO generators are used to customize the optimal carrier power level entering in each mixer.
- Power supply net, implicitly connected to both layout and schematic.
- Mixer's loads, represented by  $50\Omega$  resistors connected to unitary gain driven generator. This is used both for ideal impedance matching purposes and to convert differential (balanced) output from mixers to single-ended (unbalanced).





(a) layout



(b) schematic

**Figure 27:** Discrete Fourier transform: double balanced differential output with  $v_{RF}=200\text{mV}$ ,  $f_{RF}=110\text{MHz}$ ,  $v_{RF}=1.23\text{mV}$ ,  $f_{LO}=100\text{MHz}$ , cosine squared smoothing function. a) layout, b) schematic

## 6.2 Time domain mixed signal

The mixed output signal with  $v_{rf}=200\text{mV}$  and  $v_{lo}=1.23\text{V}$  is visible in figure 24. The waveform looks like the expected one from literature (**REFERENCE**). Applying the discrete Fourier transform to the if signal we found the graph seen in figure 27a and 27b. It's clearly visible the intrinsic capability of double balanced mixer of rejecting input components at  $v_{lo}=100\text{MHz}$  and  $v_{rf}=110\text{MHz}$ .

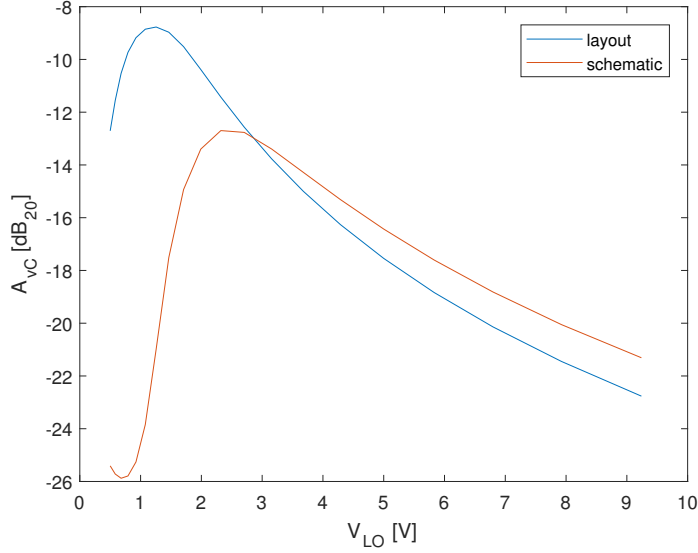


**Figure 28:** Conversion gain vs  $V_{LO}$ .

### 6.3 Maximum conversion gain vs LO

Input LO signal was swept to find the optimum value that maximizes output voltage at IF. The analysis has been carried on for both schematic and layout circuit. Voltage  $v_{rf} = 200mV$  was kept constant during the analysis, and output amplitude at 10MHz was divided by LO amplitude such that the peak corresponds to the maximum LO amplitude for which IF output power saturates. Results are shown in figure 28. It can be noticed that schematic and layout reach their maximum for different values of LO signal, 2.5V and 1.23V respectively. In general it can be noticed that layout has an higher gain than the schematic. Trying to change  $v_{rf}$  amplitude very tiny changes in peak output voltage where found, so the first analysis was kept as a quite good estimation for optimum LO peak voltage. From now on all the comparison between the two circuits have been made imposing the optimum LO voltage for each circuit.

### 6.4 Conversion gain and 1dB compression point

Keeping optimum LO amplitude, RF's voltage was swept in order to see how output power at IF frequency increases with input power at RF. Reference port for all power measurement has been chosen to be  $50\Omega$ .  $P_{IF}$  as a function of  $P_{RF}$  conversion gain is shown in figure 29 for both schematic and layout, whereas gain can be seen in figure 30.



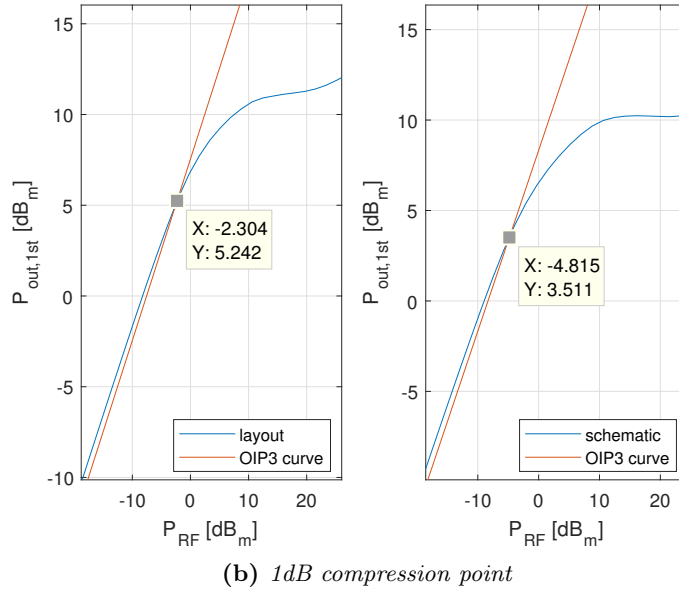
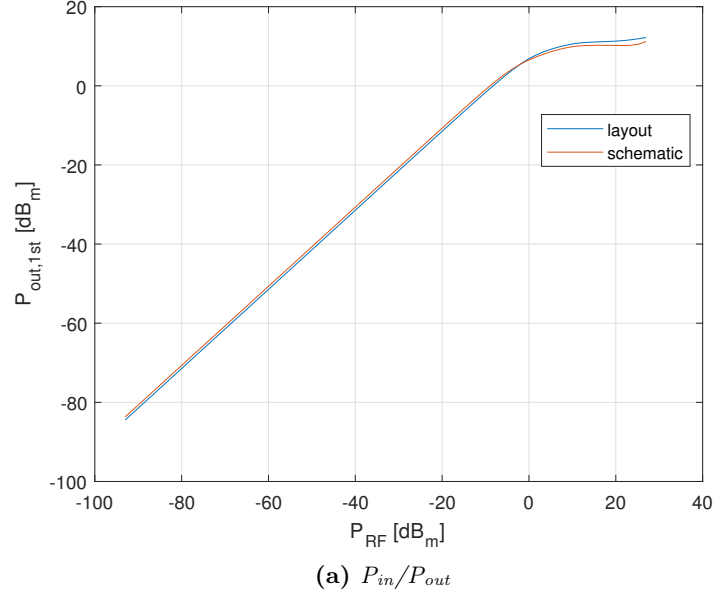


**Figure 29:** a)  $P_{in}/P_{out}$  and b) 1dB compression point, one-tone analysis.

From simulation we have:

$$G_C|_{layout} = 4.27dB \Rightarrow A_{vC}|_{layout} = 2.67$$

$$G_C|_{schematic} = 4.88dB \Rightarrow A_{vC}|_{schematic} = 3.08$$

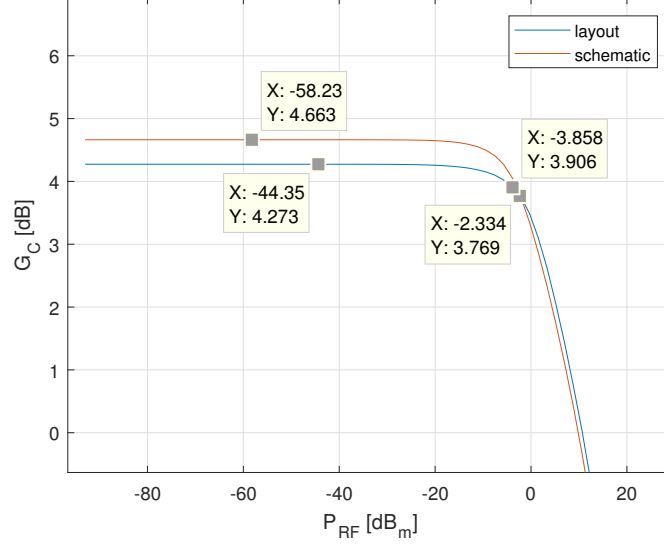


**Figure 30:** Conversion gain vs  $v_{RF}$ .

Extrapolation of 1dB compression point was carried on, leading to the measurement of RF power for which the gain drops of 1dB equal to

$$P_{RF,in}|_{layout} = 5.24dB_m$$

$$P_{RF,in}|_{schematic} = 3.51dB_m$$

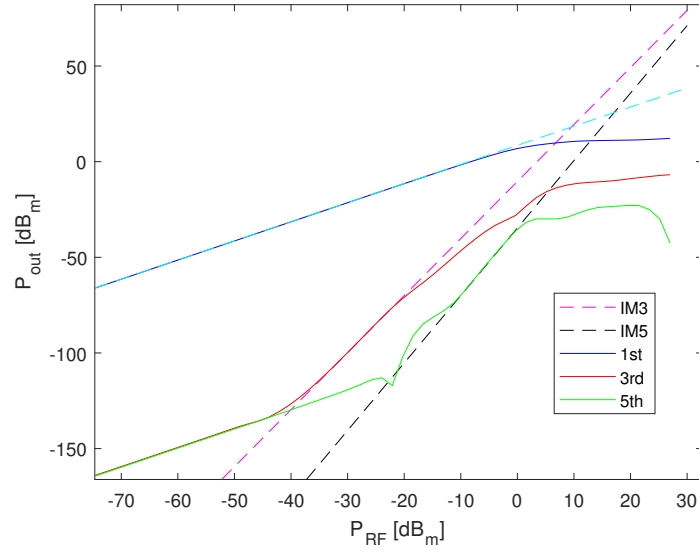
then, respectively for schematic and layout, corresponding to the voltages:

$$V_{RF,in}|_{layout} = 122.3mV$$

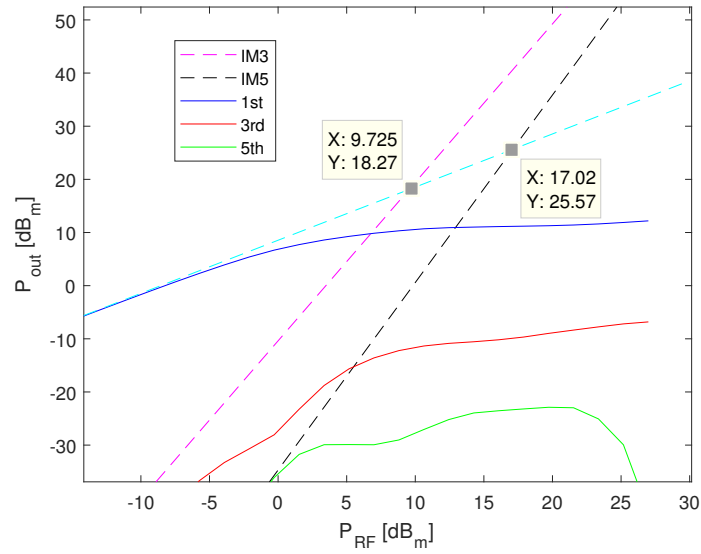
$$V_{RF,in}|_{schematic} = 149.2mV$$

## 6.5 Single tone third order distortion

Using single tone RF signal, power on the third harmonic with respect to the IF tone has been measured. Third order distortion is in fact the first contribution to non-linearities(**SELFREFERENCE**). The typical cubic behaviour with respect to the linear one of the conversion gain can be easily seen in logarithmic scale, shown in figure 31 for the schematic and in figure 32 for the layout. Linear regression was applied to the curves to find the third order intercept points for both schematic and layout test benches. Values of IIP3 and OIP3 thus found for both layout and schematic are reported in table 2. From where it appears that the layout extracted introduces less third order distortion than schematic, fifth order distortion looks higher at lower input power though.



(a) harmonics power



(b) detail in  $IIP_3$  and  $IIP_5$

**Figure 31:** Harmonics power,  $IIP_3$  and  $IIP_5$  in schematic, one tone analysis.

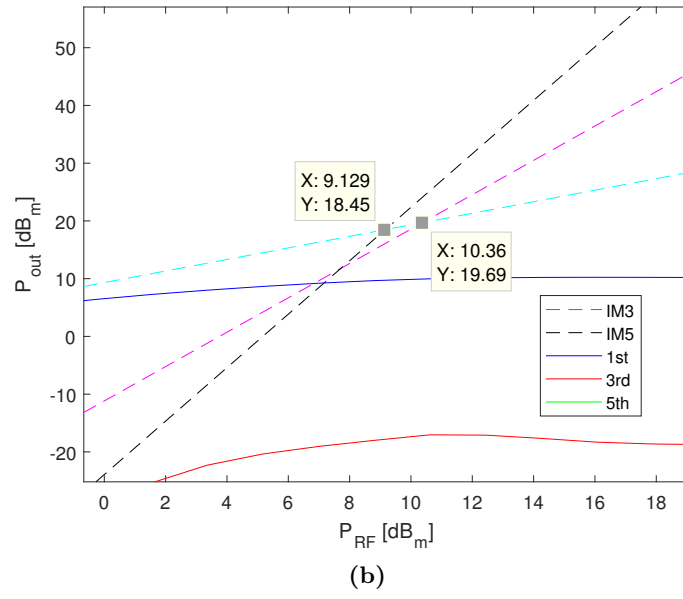
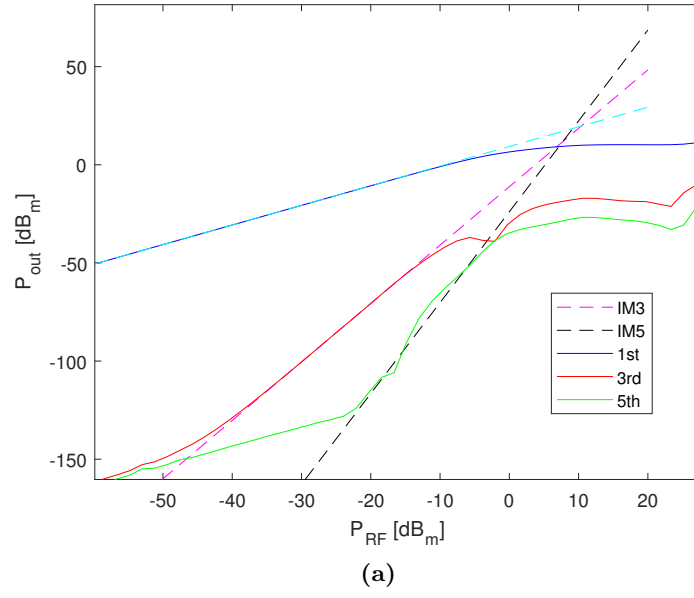


**Figure 32:** IIP<sub>3</sub> and IIP<sub>5</sub> in layout, one tone analysis.

**Table 2:** IIP3 and IIP5 in one tone analysis.

| Parameter Name | Schematic | Layout | unit          |
|----------------|-----------|--------|---------------|
| $IIP_3$        | 9.73      | 10.4   | $\text{dB}_m$ |
| $OIP_3$        | 18.3      | 19.7   | $\text{dB}_m$ |
| $IIP_5$        | 17.0      | 9.13   | $\text{dB}_m$ |
| $OIP_5$        | 25.6      | 18.5   | $\text{dB}_m$ |

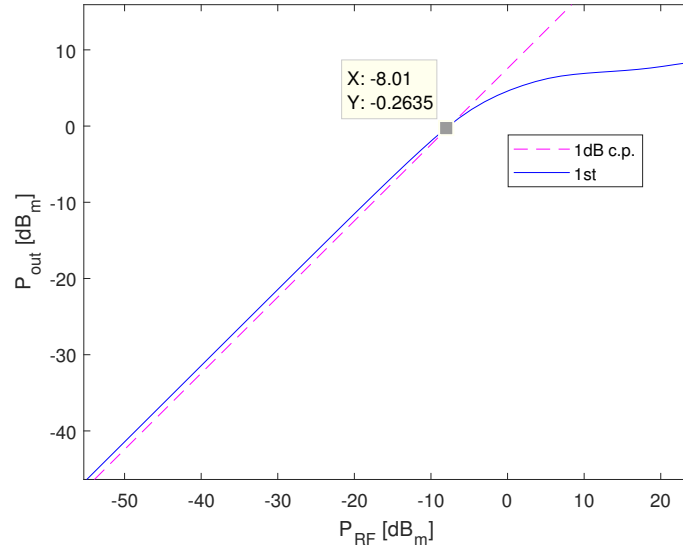
### 6.6 Two tone $IM_3$ and $CIM_3$ ratio

In order to simulate the behaviour of a non-monochrome, fixed-bandwidth signal, the two tone analysis has been carried on. Two RF tones at  $f_{RF}=110\text{MHz}$  and  $f_{RF}'=f_{RF}+\delta f=111\text{MHz}$  have been adopted. Figure 33 shows the 1dB compression point in this case. Third order intermodulation frequency components result to be at  $9\text{MHz}$  and  $12\text{MHz}$ . Their behaviour along with increasing input power is shown in figure 34a and 34b. Graphs show that power related to fundamental is strongly reduced when two tones are injected, since power is equally spread among them. From simulation appears that the  $IIP_3$  is reduced by roughly three dB, accordingly to the doubled power injected due two tones.

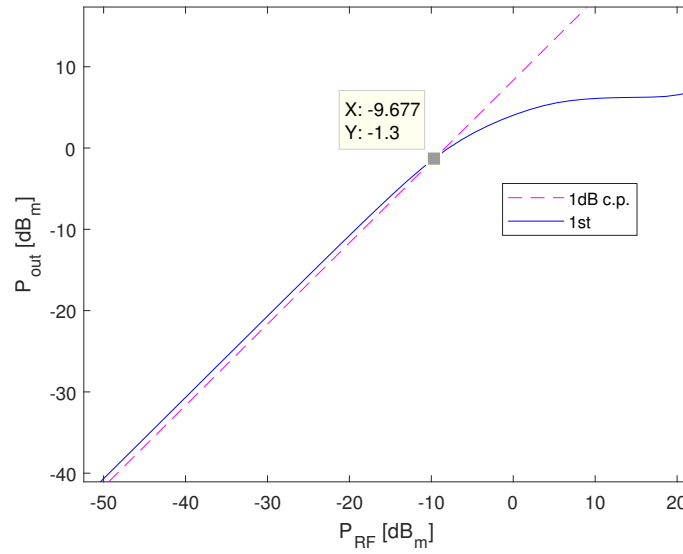
Frequency spectra at difference input power are shown in figure 35 and 36. From the latter, informations about the carrier to third intermodulation data are selected. In particular, the 1dB compression point spectrum has been chosen ( $P_{RF}=-9.68\text{dB}_m$ ), since this is set as the maximum input power accepted by the multiplier without heavy distortion. As it appears, power carried from fundamental tones (10MHz and 11MHz) barely increases after this point, whereas other tones keep increasing. Overall, the layout looks less performing as expected.

**Table 3:** 1dB compression point, IIP3 and CIM3 in two tones analysis.

| Parameter Name | Schematic | Layout | unit          |
|----------------|-----------|--------|---------------|
| $P_{RF,1dB}$   | -8.01     | -9.68  | $\text{dB}_m$ |
| $IIP_3$        | 8.42      | 5.06   | $\text{dB}_m$ |
| $OIP_3$        | 16.9      | 14.4   | $\text{dB}_m$ |
| $CIM_{3,1dB}$  | 16.7      | 14.1   | dB            |

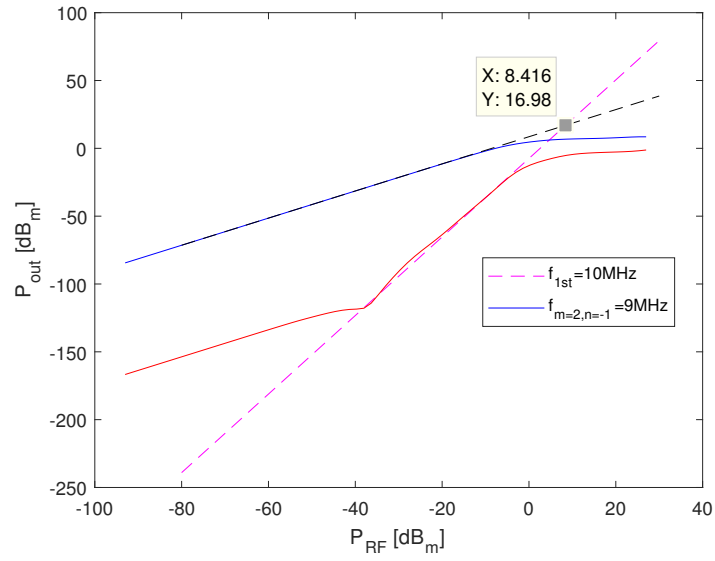


(a) *schematic*

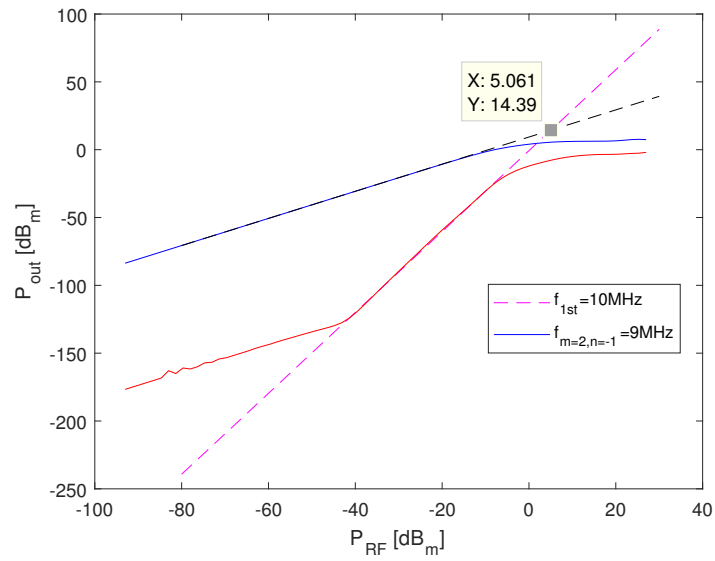


(b) *layout*

**Figure 33:** 1dB compression point, two tones.

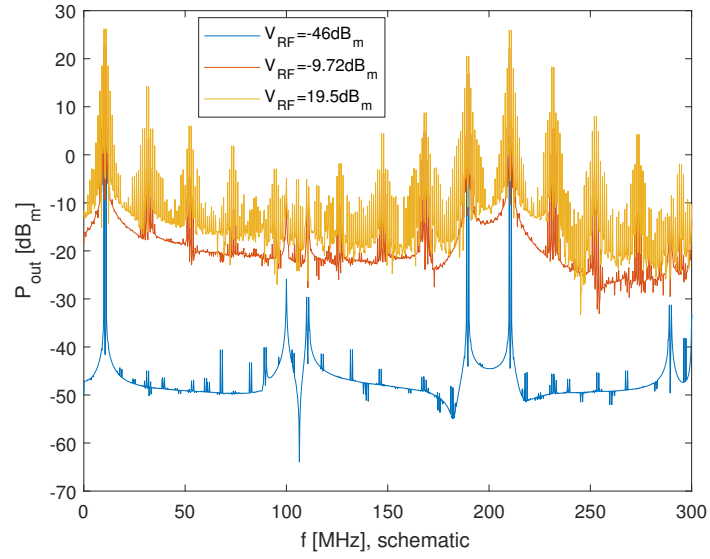


(a) *schematic*

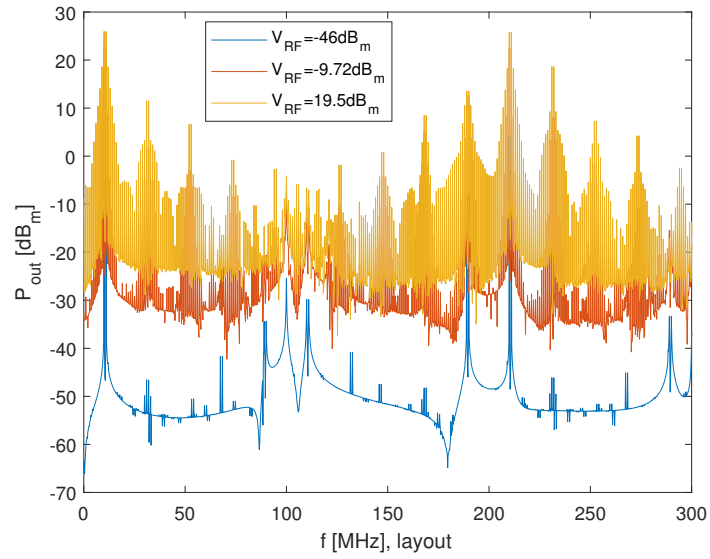


(b) *layout*

**Figure 34:** Harmonics power,  $IIP_3$  and  $IIP_5$  in schematic, two tone analysis.



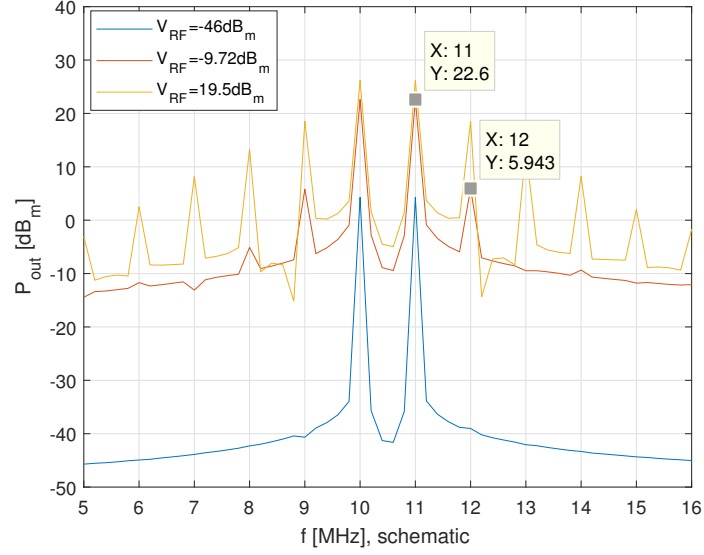
(a) *schematic*



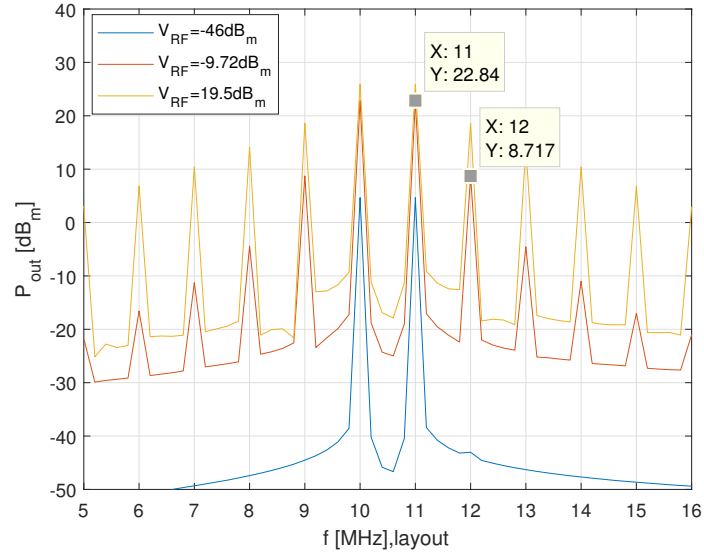
(b) *layout*

**Figure 35:** DFT, comparison between layout and schematic; cosine2 smoothing function.





(a) *schematic*



(b) *layout*

**Figure 36:** DFT, comparison between layout and schematic. CIM<sub>3</sub> measurement at 1dB compression point; cosine2 smoothing function.

## 6.7 Bandwidth and CMRR of RF stage (output node filtering, current mixing)

In order to have an estimation of what the maximum operating frequency of the mixer could be, an ac analysis on the differential RF stage has been

made, keeping LO stage fixed in bias condition. The analysis led to the bode plot seen in

FIGURA

, which shows a  $-3dB$  bandwidth of approximately  $113MHz$ , and a common mode rejection ratio of

dB

. Our assumptions on LO and RF frequencies were thus considered adequate, since represent the worst-case performances of the mixer. Moreover it has to be noticed that the mixing operation is done on the RF current. Maximum operating frequency could thus be improved reducing output node capacitance.

## 6.8 pavarotti?

## 7 Conclusions